ACS OMEGA

Open Access

http://pubs.acs.org/journal/acsodf

Article

Enhancing the Mechanical Properties of Electrospun Poly(3-hydroxybutyrate-*co*-3-hydroxyvalerate) Fiber Mats Using Deep Eutectic Solvents

Ahmet O. Basar, Cristina Prieto,* Luis Cabedo, and Jose M. Lagaron*

Cite This: *ACS Omega* 2025, 10, 12936−12952

Read Online

ACCESS | Metrics & More | Article Recommendations | Supporting Information

ABSTRACT: In this study, the use of deep eutectic solvents (DESs) was considered for the first time to improve the mechanical properties of electrospun poly(3-hydroxybutyrate-*co*-3-hydroxyvalerate) (PHBV) fiber mats. For this, different DES formulations, namely, Choline Chloride (ChCl):Urea:Water, ChCl:Glycerol (Gly), and Gly:Sodium Citrate (NaCitrate), were selected and evaluated at a concentration of 10 wt %, and their efficacy enhancing mechanical properties was compared against traditional plasticizing additives glycerol and acetyl tributyl citrate (ATBC). The impact of these formulations on PHBV fiber mats was evaluated in terms of thermal, crystallinity, and mechanical properties, both as obtained and after aging. All samples produced macroscopically consistent, self-supporting, and handleable nonwoven material sheets. The DES-containing PHBV showed a thinner, bead-free surface morphology but a rugose surface morphology. DSC results indicated that glycerol, ATBC, and Gly:NaCitrate (DES) exhibited the highest reduction in melting temperatures, with a notable 5.6 °C decrease for the mat containing Gly:NaCitrate. Interestingly, electrospun PHBV fibers containing DES revealed a larger quantity of β-form planar zigzag chain conformations, so-called β-form crystals. Tensile test results revealed that depending on the additive formulation, the mechanical performance of the samples was fundamentally different from each other. Among DESs, PHBV fiber mats with ChCl-based DES were excessively brittle. Surprisingly and interestingly, PHBV fiber mats containing Gly:NaCitrate exhibited an unreported significant increase in all mechanical properties, including modulus, elongation at break, and toughness. Overall, this study highlights the potential of DESs as unique additives to tailor the mechanical properties of electrospun PHBV materials.

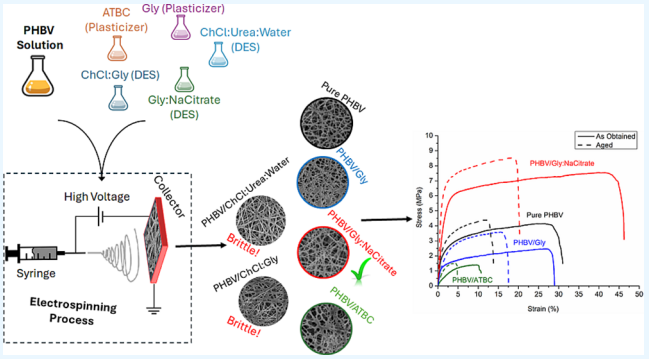

1. INTRODUCTION

Deep eutectic solvents (DESs), first introduced in 2003 by Abbott et al.,[1] can be defined as eutectic mixtures of a hydrogen bond acceptor (HBA) and hydrogen bond donor (HBD), which form a homogeneous mixture that remains liquid at temperatures significantly below the melting points of its individual constituents and their ideal mixtures.[2,3] As DESs consist of two (or more) components, their properties are highly tunable and can display sought-after features, such as a wide range of polarity, liquid state far below 0 °C, high solubilization and stabilization capacity for a broad range of compounds, high extraction performance, and many more.[4−6] Furthermore, depending on their constituents, DESs can be excellent alternatives to the traditional organic solvents, offering environmentally benign properties such as low cost, biodegradability, biocompatibility, easy production, and non- or low toxicity.[5] Another great potential of DESs lies in their capability to liquefy compounds targeted for specific applications that would otherwise remain solid and unsuitable for use in liquid form at the desired temperature.[6] Due to these wide range of properties, DESs have attracted a lot of attention from numerous applications and research areas, including organic synthesis, extraction and separation,[7] gas capture,[8] electrochemistry, biosensors, biocatalysis,[5] and many more.[9] DESs have also been utilized for modifying the mechanical properties of polymeric systems, including cellulose,[10] starch,[11] and chitosan,[12] and also other different types of polymers, including zein.[13]

Among biopolyesters, polyhydroxyalkanoates (PHAs) represent one of the most promising families of biopolymers for the substitution of conventional petrochemical-based polymers. PHAs are produced by a wide range of microorganisms and have excellent biodegradability and biocompatibility characteristics.[14] Among PHAs, one of the most studied copolymer is

Received: October 1, 2024
Revised: December 16, 2024
Accepted: January 16, 2025
Published: March 28, 2025

poly(3-hydroxybutyrate-*co*-3-hydroxyvalerate) (PHBV) composed of the homopolymer poly(3-hydroxybutyrate) (PHB) with hydroxyvalerate (3HV) units along the backbone.[4] Commercial PHBV is currently limited to low 3HV contents (<12 wt %) that lead PHBV to present relatively similar characteristics to those of the homopolymer.[15] Both PHB and PHBV having low 3HV contents are highly stiff and brittle materials due to their high stereoregularity, high degree of crystallinity, macromolecular organization, and formation of very large and overlapped spherulites with a high tendency to crack.[16−18] They typically exhibit low toughness and ductility, which hinder their applications.[19] Another drawback, which applies to all PHA-based homopolymers and copolymers, is that their glass transition temperature (T_g) is close to room temperature. This proximity leads these polymers to be prone to embrittlement, which decreases their ductility and increases their stiffness and brittleness.[18,20] Furthermore, another significant limitation is their narrow processing window originating from their low resistance to thermal degradation.[21]

Many attempts have been made to overcome the previously mentioned drawbacks of PHAs by adding a variety of compounds to modify their characteristics such as plasticizers or toughening agents. The selection of additives should be meticulously done because their efficiency depends on their compatibility with the host polymer, which is mainly polarity, molecular size or weight, and shape driven.[22] To our knowledge, many substances have been utilized to modify the mechanical behavior PHB and PHBV, such as citrate esters,[19,21,23−27] glycerol/derivatives,[23,24,28,29] phthalates,[25−27] fatty acids/esters,[30] vegetable oils,[23−26] and oligomeric plasticizes such as poly(ethylene glycol).[16,23,24,28]

Additionally, studies on modulating the mechanical properties of PHAs generally involve processes such as melt blending,[16,18,19,23,24,30] compression molding,[21,28,29,31] or solvent casting.[28] However, PHAs processed using these techniques often exhibit low flexibility and toughness, especially after the secondary crystallization occurs.[23,32−34] Additionally, these processing methods subject the polymer to elevated pressures, high deformation rates, and rapid cooling, all of which influence crystallization and strongly affect the final material. In this regard, the electrospinning technique is an innovative alternative for PHA processing. Electrospinning involves the rapid evaporation of liquid polymeric solutions due to an applied high electrical potential, generating lower-crystallinity micro- or nanofiber mats at room temperature.[35] Recent advancement in scalable electrospinning systems, including multineedle and needleless configurations, further enhance its potential for high-throughput production without compromising fiber quality.[36] This technique enables polymers to exhibit unique morphological, structural, and mechanical features, while room-temperature processing prevents the thermal degradation of PHAs.[37] To date, only a limited number of studies have investigated the incorporation of DES into biobased polymers using traditional melt mixing[38] and extrusion methods.[39] However, no attempts have been made to modify the mechanical properties of PHAs using DES through an electrospinning technique.

In this context and to the best of our knowledge, modulating the PHAs' mechanical behavior through the combined use of DESs and the electrospinning technique remains unexplored. The main objective of this work was to evaluate the effectiveness of different DES formulations in the properties of PHBV. Thus, various DESs were formulated and loaded into electrospun PHBV fibers and, for the first time, characterized in terms of their morphology, thermal properties, crystallinity, and mechanical performance. Additionally, the impact of DESs was compared with that of two conventional plasticizing additives, i.e., glycerol and ATBC.

2. MATERIALS AND METHODS

2.1. Materials. Commercial poly(3-hydroxybutyrate-*co*-3-hydroxyvalerate) (PHBV), ENMAT Y1000P, was purchased from Tianan Biologic Materials (Ningbo, China) and delivered in the form of pellets. According to the manufacturer, the density and molecular weight (Mw) of the biopolymer resins were 1.23 g/cm^3 and approximately 2.8 × 10^5 g/mol, respectively. The 3HV fraction in the copolyester was 2−3 mol %.

2,2,2-Trifluorethanol (TFE) (≥99%) was purchased from Merck (Darmstadt, Germany). Choline chloride (ChCl) (≥98%), urea (≥99%), and acetyl tributyl citrate (ATBC) (≥98%) were purchased from Sigma-Aldrich (St. Louis, MO, USA). Glycerol (Gly) (pure, pharma grade) was obtained from AppliChem GmbH (Darmstadt, Germany). Sodium citrate tribasic hydrate (NaCitrate) (purity of ≥99%) was purchased from Honeywell, Riedel-de Haen (Charlotte, NC, USA). Distilled water was used throughout the study.

2.2. Preparation of Deep Eutectic Solvents. Deep eutectic solvents (DESs) were prepared in a molar ratio of two different components consisting of a hydrogen bond donor (HBD) and a hydrogen bond acceptor (HBA). Prior to use, choline chloride (ChCl) was dried at 65 °C under a vacuum (Vaciotem-T, JP Selecta, Barcelona, Spain) for 24 h to remove any possible moisture. Three different deep eutectic solvents—ChCl:Urea:Water, ChCl:Gly, and Gly:NaCitrate—were prepared by weighting the individual components in appropriate mole ratios of 1:2:1, 1:2, and 15:1, respectively, as these are the most commonly reported in the literature.[4,40,41] The mixtures were then heated under constant stirring at 80 °C until a clear, colorless liquid was obtained. The prepared DESs remained in the liquid state after cooling to room temperature for several months and were stored in the desiccator until further use.

2.3. Solution Preparation. Electrospinning solutions were prepared by dissolving 10 wt % of PHBV in TFE at 50 °C through gentle stirring overnight. Thereafter, prepared DESs were added individually to PHBV solutions to attain a final DES-to-PHBV ratio of 10 wt %. The resultant mixture was homogenized using a TX4 Digital Vortex Mixer from Velp (Usmate, Italy). For comparison purposes, ATBC and pure glycerol were used as plasticizing controls because they are conventional plasticizers for PHBV. The control samples were prepared at the same concentration and following the same preparation protocol. To assess the effect of DES concentration on the fiber morphology, PHBV solutions were prepared with ChCl:Urea:Water with a DES-to-PHBV ratios of 10, 25, and 55 wt %.

2.4. Solution Characterization. Prior to electrospinning, polymeric solutions were characterized in terms of their conductivity, viscosity, and surface tension. The conductivity measurements were carried out using a Hanna Instruments HI98192 conductivity probe (Gothenburg, Sweden). The viscosity was measured using a Fungilab Visco Basic Plus (Barcelona, Spain). Finally, the surface tension measurements were done using the Wilhelmy plate method in a Kruss GmbH EasyDyne K20 tensiometer (Hamburg, Germany). All of the measurements were carried out in triplicate at room temperature.

https://doi.org/10.1021/acsomega.4c08969
ACS Omega 2025, 10, 12936−12952

2.5. Electrospinning. The electrospinning apparatus used was the Fluidnatek LE-10 electrospinning benchtop equipment from Bioinicia S.L. (Valencia, Spain) featuring a variable high-voltage power supply (0−30 kV) and a motorized scanning injector. The electrospinning solutions were transferred to a 20 mL plastic syringe and coupled by a tube to a stainless-steel needle (internal diameter of 0.4 mm) that was connected to the power supply. The distance between the needle and collector was optimal at 15 cm. Pure PHBV and ATBC- and glycerol-containing PHBV fiber mats were obtained using a voltage of 14 kV and a flow rate of 6 mL/h. For the case of PHBV fibers containing DES, the optimal voltage and the flow rate were 20 kV and 3 mL/h, respectively. The electrospinning process was performed at a relative humidity (RH) level of 50% and at room temperature. The operation parameters were optimized for each formulation to obtain a stable Taylor cone, which ensures stable processing. The resultant electrospun fiber mats were labeled as follows: pure PHBV, PHBV/Gly, PHBV/Gly:NaCitrate, PHBV/ChCl:Gly, PHBV/ATBC, and PHBV/ChCl:Urea:-Water, each with the respective additives at a concentration of 10 wt %. In all cases, the obtained electrospun materials were stored in a desiccator at room temperature and 20% relative humidity until further use.

2.6. Characterizations. *2.6.1. Morphological Characterization.* The morphology of the electrospun fibers was examined by scanning electron microscopy (SEM) in a Hitachi S-4800 electron microscope (Tokyo, Japan) at an accelerating voltage of 5 kV and a working distance of 8 mm. Prior to observation, the samples were fixed to holders using conductive double-sided adhesive tape and sputtered with a mixture of gold−palladium for 2 min under vacuum. The average fiber diameter and porosity were determined via the ImageJ Launcher software program (National Institutes of Health (NIH), Bethesda, MD, USA) from the SEM micrographs in their original magnifications. Porosity was estimated as the ratio of the porous area to the total area of the mat as previously described.[42]

2.6.2. Differential Scanning Calorimetry (DSC). Thermal transitions of the studied samples were analyzed by DSC using the Q20 equipment from TA Instruments (New Castle, DE, USA) under a nitrogen atmosphere. Approximately 3 mg of the sample was placed into a Tzero hermetic aluminum pan and sealed. For the electrospun PHBV fiber mats containing DES and pure glycerol, the samples were predried at 100 °C, whereas no predrying step was used for pure PHBV and PHBV/ATBC fiber mats. The thermal runs were then performed as a first heating step from −20 to 190 °C. All of the runs were set to 10 °C/min. The DSC equipment was previously calibrated with indium as a standard, and the slope of thermograms was corrected by subtracting similar scans of an empty aluminum pan. The enthalpy of melting (ΔH_m) values were corrected according to the weight fraction of PHBV in the sample. Each sample was measured only once, and all thermograms were analyzed using the TA Universal Analysis 2000 software (TA Instruments, New Castle, DE, USA).

2.6.3. WAXS and SAXS Analysis. Simultaneous wide-angle X-ray scattering (WAXS) and small-angle X-ray scattering (SAXS) experiments were carried out on beamline BL11−noncrystalline diffraction (NCD) (WAXS/SAXS station) located at the ALBA synchrotron facilities (Barcelona, Spain). The WAXS and SAXS q-axis calibrations were obtained by measuring chromium(III) oxide (Cr_2O_3) and silver behenate ($AgC_{22}H_{43}O_2$) standards, respectively. Scattering patterns were collected using the combination of two detectors, that is, a photon counting Pilatus 1M detector from Dectris AG (Baden, Switzerland) and a CDD WAXS LX255-HS detector from Rayonix, L.L.C. (Evanston, IL), operating simultaneously in the SAXS and WAXS positions, respectively. The wavelength of the incident radiation (λ) was 1 Å. The distances between the sample and the WAXS and SAXS detectors were set at 0.0941 and 6.6582 m, respectively, allowing a q-range between 3.63 and 91.9 nm^{-1} for WAXS and a q-range between 0.0246 and 2.2480 nm^{-1} for SAXS. The beamline delivered a photon flux onto the sample of $>1.5 \times 10^{12}$ ph·s^{-1} at 12.4 keV for a beam current of 150 mA with a bandpass ($\Delta E/E$) of 2.7×10^{-4} at 10.0 keV and a beam size at sample position of 349 × 379 μm. For the experiments, electrospun mats, with a thickness of 100 μm, were placed on a THMS600 from Linkam Scientific Instruments Ltd. (Epstom, UK) set at 25 °C. The width of a crystal lattice, estimating the minimal possible size of crystals, for the selected Bragg reflections was determined using the Scherrer equation (eq 1):

$$D = \frac{k \cdot \lambda}{\beta \cdot \cos \theta} \quad (1)$$

where k is the shape constant, λ is the wavelength of incident radiation, β is the full width at half-maximum intensity< and θ is the Bragg angle.

2.6.4. Mechanical Characterization. Mechanical properties of the electrospun samples were determined according to ASTM D638 using a 4400 device from Instron (Norwood, MA, USA). The tests were performed under room conditions (50% RH, 24 °C) using microtraction samples (5 × 25 mm). Samples were stretched along one (machine) direction at a constant cross-head speed of 10 mm/min. All of the tests were recorded in quintuplicate, and average values of the mechanical parameters with standard deviations were reported. PHBV fiber mats containing ChCl-based DES were too brittle for tensile testing and were therefore excluded from the analysis.

2.6.5. Aging Study. To assess the effect of the additives on the embrittlement of PHBV, both DSC and mechanical analyses were conducted on the samples as obtained (samples were analyzed within 8 h after electro-hydrodynamic processing) and after aging for 7 days. This timing was based on previous studies suggesting that the majority of the structural changes in PHA occur within the first week due to the so-called secondary crystallization processes.[43−45] For this purpose, immediately after the electrospinning process, all electrospun fiber mats were subjected to DSC and mechanical testing. Subsequently, all samples measuring approximately 10 × 20 cm^2 and 50 μm in thickness were enclosed in aluminum foil envelopes and stored at 25 °C and 5 ± 3% relative humidity (RH). After 7 days of storage, they were labeled as "aged" and reanalyzed. In the case of synchrotron WAXS and SAXS analyses, only pure PHBV fiber mats were evaluated as obtained, while all other samples were analyzed as "aged".

2.7. Statistical Analysis. One-way analysis of variance (ANOVA) followed by a multiple comparison test (Tukey) with 95% significance level was performed to determine the statistical differences using the software OriginPro8 (OriginLab Corporation, Northampton, MA, USA). For analyses, $p \leq 0.05$ was considered statistically significant.

3. RESULTS AND DISCUSSION

3.1. Selection and Concentration of DESs. The selection criteria for deep eutectic solvents (DESs) were designed to explore the following question: "How do the individual

https://doi.org/10.1021/acsomega.4c08969
ACS Omega 2025, 10, 12936−12952

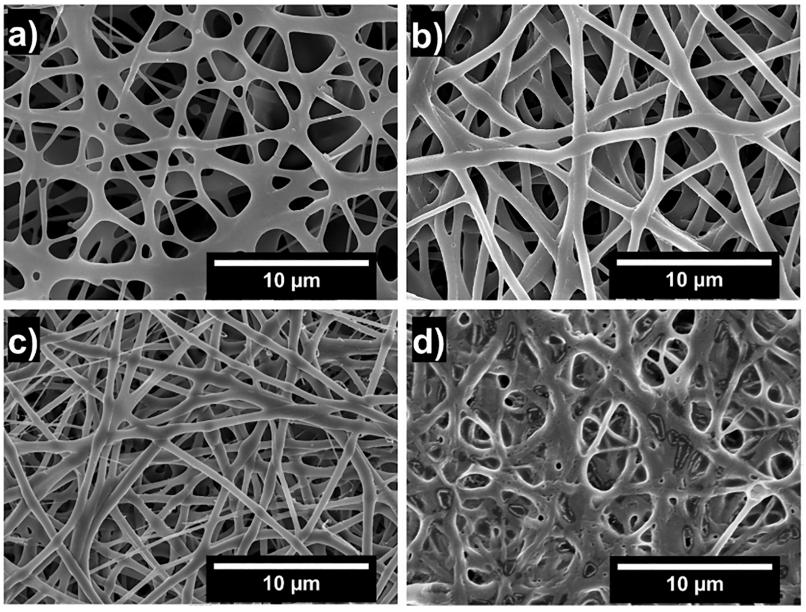

Figure 1. Scanning electron microscopy (SEM) images of the electrospun poly(3-hydroxybutyrate-*co*-3-hydroxyvalerate) (PHBV) fibers containing different concentration of DES: (a) 0 wt %, (b) 10 wt %, (c) 25 wt %, and (d) 55 wt %.

components of DES influence its mechanical performance?" This inquiry is pivotal because, in our view, DESs should be regarded not as novel or pseudocompounds but rather as mixtures. This perspective is also supported by the review articles by Martins et al.[2] and Abranches et al.,[6] which emphasize the significance of considering DESs as compositions of their precursor elements. This distinction is crucial because the functionality of DESs is profoundly influenced by their precursor components, making them highly customizable for achieving specific functionalities in targeted applications. This perspective emphasizes the importance of understanding the interplay among the components of DESs, particularly considering the vast number of possible combinations.

1. ATBC: This additive was selected as the reference plasticizer for PHBV[46] and therefore used as a control. This selection was also motivated by the absence of literature on the plasticization of PHBV with ATBC using the electrospinning technique.
2. Glycerol (Gly): This additive was selected and utilized in its pure form as a control given its established use in PHA plasticization.[23,29] Furthermore, glycerol was chosen as a primary component for DES formulations.
3. Gly:NaCitrate: The selection of this DES[41] was based on the favorable compatibilization effect of citrate esters on PHBV.[19,21,23−27] Therefore, sodium citrate was selected as another component of DES. Although sodium citrate lacks ester groups typically associated with compatibility, it was hypothesized that its citrate backbone and carboxylate groups could provide a degree of interaction with PHBV. Additionally, the solid state of NaCitrate necessitated its liquefaction, which was achieved through the formation of DES.
4. ChCl:Gly: Choline chloride was selected as the second component for DES[40] formation. ChCl is among the most commonly used DES components, and ChCl:Gly has previously been reported as a plasticizer for polysaccharides.[10] However, no literature reports were identified regarding its applications in the plasticization of PHAs. Therefore, ChCl:Gly was investigated to assess its efficacy in the plasticization and compatibilization of PHA.
5. ChCl:Urea:Water: This DES was chosen as a model DES.[4] Similar to ChCl:Gly, ChCl:urea has been documented to act as a plasticizer for polysaccharides.[47] However, there are no reports on the use of choline chloride, urea, or their combination as a DES additive for PHA. The inclusion of a small amount of water aimed to reduce viscosity based on previous studies,[11] enhancing the DES's utility. The optimization of the fiber morphology with varying DES concentrations was carried out using the model ChCl:urea:water DES.

To ascertain a suitable DES concentration in the fiber mat, ChCl:Urea:Water was incorporated within the PHBV matrix at the different concentrations of 10, 25, and 55 wt %. Figure 1 shows the morphology of the developed PHBV/ChCl:Urea:-Water electrospun fibers at different concentrations as well as the pure PHBV fibers. Pure PHBV fibers having no DES (Figure 1a) exhibited a heterogeneous morphology, with large fused fibers and some thinner fibers interconnecting them. However, when DES was incorporated into PHBV fibers at the concentrations of 10 wt % (Figure 1b) and 25 wt % (Figure 1c), more homogeneous fibers appeared, being somewhat thicker for the 10 wt %. Interestingly, from Figure 1d and under the optimal processing conditions found, it can be observed that PHBV fibers having 55 wt % DES exhibited a gelly-like morphology with interconnected fused fibers, possibly due to the excess of the deep eutectic solvent causing insufficient solvent evaporation. Further model work in the study was decided to be carried out with the 10 wt % DES because it provided a somewhat better process stability and aligned well with plasticizer concentrations used by other authors. For instance, Martino et al. suggested an optimum plasticizer concentration of 10 wt % for melt-extruded PHBV (ENMAT Y1000P) films over 5 and 20 wt % because the best mechanical performance was reported for this concentration of plasticizers, which were ATBC, glycerol triacetate (GTA), and polyethylene glycol (PEG).[24] In another study, Jost et al. utilized a maximum

https://doi.org/10.1021/acsomega.4c08969
ACS Omega 2025, 10, 12936−12952

admissible plasticizer concentration of 13 wt % for the extrusion of PHBV (ENMAT Y1000P) films with propylene glycol (PG), glycerol (G), triethyl citrate (TEC), castor oil (CO), epoxidized soybean oil (ESO), and PEG.[23] In the former study, it was stated that the maximum plasticizer concentration depended on both the solubility in the polymer and the experimental setup of the compounding plant.

3.2. Solution Characterization. It is well-known that the electrospinnability and final morphology of the materials is dependent on the physical characteristics of the initial electrospinning solution, such viscosity, surface tension, and electrical conductivity.[48] Table 1 displays the properties of neat and 10 wt % of additive-containing PHBV solutions. All polymeric solutions exhibited roughly the same surface tension, i.e., below 40 mN/m, indicating a stable electrospinning process.[49−51] The addition of the additives provoked a decrease in viscosity in comparison with the pure PHBV solution. A slight decrease was observed for the addition of glycerol, Gly:NaCitrate, and ChCl:Gly, whereas a more prominent decrease was detected for the addition of ATBC and ChCl:Urea:Water.

Table 1. Properties of Pure and 10 wt % Additive-Containing PHBV Solutions[a]

solutions	viscosity (cP)	surface tension (mN/m)	conductivity (μS/cm)
pure PHBV[b]	571.5 ± 2.1[a]	21.2 ± 0.1[d]	4.0 ± 0.0[c]
PHBV/ATBC	469.1 ± 3.7[e]	22.2 ± 0.1[b,c]	3.8 ± 0.0[c]
PHBV/Gly	556.1 ± 3.1[b]	22.3 ± 0.1[c]	2.5 ± 0.0[c]
PHBV/ Gly:NaCitrate	563.3 ± 2.8[a,b]	22.4 ± 0.1[c]	16.3 ± 1.2[c]
PHBV/ChCl:Gly	528.4 ± 4.1[c]	21.9 ± 0.1[c]	797 ± 22[b]
PHBV/ ChCl:Urea:Water	482.2 ± 1.8[d]	22.8 ± 0.1[a]	880 ± 18[a]

[a]Different letters in the same column indicate a significant difference among the samples ($p < 0.05$). [b]Data reported in a previous study.[4]

However, an evident difference was observed in terms of the solution conductivity. The conductivity of the pure PHBV solution increased significantly, up to 880 ± 18 μS/cm with the addition of ChCl-based DES. In fact, in our previous study, where ChCl:Urea:Water was incorporated into a PHBV solution at a higher concentration of 26 wt % compared to this study, the solution conductivity was measured at 2595 ± 31 μS/cm[4]. Additionally, when comparing viscosity and surface tension, the latter remained consistent at 22.8 ± 0.1 mN/m, while the viscosity was lower at 442.2 ± 1.8 cP. These changes are likely due to the added compound (ChCl:Urea:Water) having a higher conductivity and lower viscosity compared to the solution in which it was incorporated.[4]

In the case of the addition of Gly:NaCitrate, this increase was not as intense as the one produced by the other DES, 16.3 ± 1.2 μS/cm, whereas the addition of ATBC and glycerol did not alter the conductivity significantly. The increase in conductivity was mainly attributed to the presence of ionic compounds forming DES because, depending on the formulation, DES could

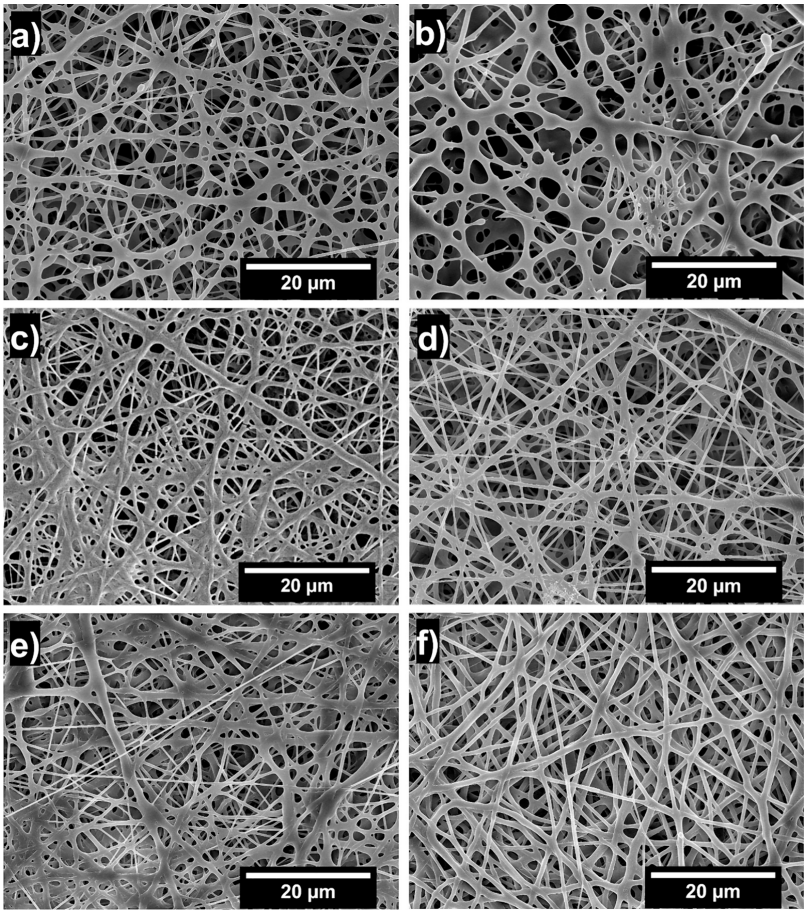

Figure 2. Scanning electron microscopy (SEM) images of the electrospun poly(3-hydroxybutyrate-co-3-hydroxyvalerate) (PHBV) fibers of (a) pure PHBV, (b) PHBV/ATBC, (c) PHBV/Gly, (d) PHBV/Gly:NaCitrate, (e) PHBV/ChCl:Gly, and (f) PHBV/ChCl:Urea:Water. All samples were analyzed in their aged condition.

https://doi.org/10.1021/acsomega.4c08969
ACS Omega 2025, 10, 12936−12952

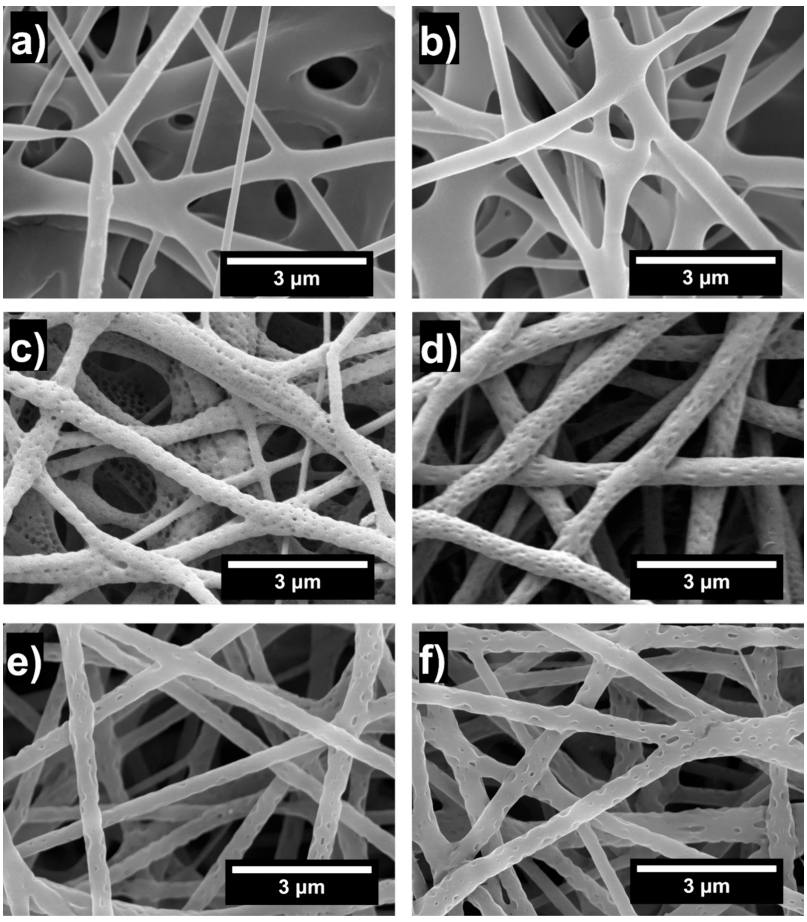

Figure 3. Scanning electron microscopy (SEM) images at higher magnification of the electrospun PHBV fibers of (a) pure PHBV, (b) PHBV/ATBC, (c) PHBV/Gly, (d) PHBV/Gly:NaCitrate, (e) PHBV/ChCl:Gly, and (f) PHBV/ChCl:Urea:Water. All samples were analyzed in their aged condition.

potentially possess higher conductivities in the range of 100 to 12,000 μS/cm^3. Additionally, Abbott et al.[52] reported that by increasing the amount of salt in the DES composition, the conductivity increases. This could be the reason for the relatively low conductivity of Gly:NaCitrate DES compared to other DESs since the molar ratio of NaCitrate was relatively lower (Gly:NaCitrate 15:1).

3.3. Morphology. All samples produced macroscopically consistent, self-supporting, and handleable nonwoven material sheets. Figure 2 shows the SEM images of the pure PHBV, PHBV/ATBC, PHBV/Gly and PHBV/DES electrospun fiber mats on their aged condition, while Figure S1 illustrates the corresponding fiber size distributions. Notably, the morphology of the as-obtained samples was consistent with the aged ones, showing no significant changes over time (results not shown). As can be seen from the figure and under the processing conditions used, pure PHBV produced, as discussed above, smooth, interfused highly cross-linked and random oriented fibers, with a mean fiber diameter of 864 ± 327 nm. The morphology and average fiber diameter of pure PHBV fibers reported here are consistent with those observed in our previous study.[4] A highly interfused thicker and random fiber morphology but with some broken fibers terminating in beads was observed for PHBV/ATBC fibers with an average size of 1201 ± 657 nm. When glycerol was added, a heterogeneous morphology with thinner fibers and some fiber-fused areas was seen but with a decreased fiber diameter of 691 ± 193 nm. A trend of decreasing fiber diameter was also observed for the DES-containing PHBV fibers when compared with pure PHBV fibers. The obtained diameters were 635 ± 272, 606 ± 253, and 670 ± 189 nm for PHBV/Gly:NaCitrate, PHBV/ChCl:Gly, and PHBV/ChCl:Urea:Water, respectively. In fact, this trend aligns with our previous study involving the electrospinning of PHBV fibers containing 26 wt % ChCl:Urea:Water, where the average fiber diameters were much thinner for the DES-containing sample than for pure PHBV.[4] As we discussed in the cited study, this can be attributed to the higher electrical conductivities of the DES-containing electrospinning solutions (Table 1) because it has been reported that the average fiber diameter decreases with increasing electrospinning solution conductivity.[53] Among the DES-containing fibers, PHBV/Gly:NaCitrate fibers (Figure 2d) showed a more homogeneous morphology with no apparent thick or interfused fiber areas compared to other ChCl-based DES-containing fibers. Notably, this fiber mat also featured some thinner, long crossing and oriented fibers, also seen in the PHBV/ChCl:Gly system, than those observed in other mats.

The average porosity of the fiber mats was also estimated from the corresponding SEM images. It can also be observed visually from Figure 2 that pure PHBV, PHBV/ATBC, and PHBV/Gly:NaCitrate fibers appear to exhibit somewhat higher porosities than those of PHBV/Gly, PHBV/ChCl:Gly, and PHBV/ChCl:Urea:Water fibers. The porosities were quantified as 45, 48, and 43% for the first group and 33, 31, and 36% for the second group, respectively.

https://doi.org/10.1021/acsomega.4c08969
ACS Omega 2025, 10, 12936−12952

It is interesting to observe that with greater magnification and resolution (see Figure 3), the surface morphology of pure PHBV and PHBV/ATBC fibers appeared smooth, whereas the PHBV fibers containing pure glycerol (Figure 3c), Gly:NaCitrate (Figure 3d), ChCl:Gly (Figure 3e), and ChCl:Urea:Water (Figure 3f) displayed a rugose surface morphology. Our previous study also demonstrated that PHBV fibers having 26 wt % ChCl:Urea:Water exhibited hollowed morphologies across the fiber cross section attributed to the presence of highly dispersed and distributed small DES segregated domains along and within the fibers.[4] From the above morphological results, it is inferred that ATBC is homogeneously mingled with the polymer amorphous phase at a molecular level, as expected and reported earlier,[24,27] whereas glycerol[23,29] and DES formed highly dispersed but segregated domains. Another observation is that the mat containing PHBV/Gly:NaCitrate appeared to show fewer fiber junctions or cross-linked areas than the other samples, the fibers being under higher magnification rather than crossing each other with some fused contact points.

3.4. Thermal Properties. The thermal properties of the additive-containing PHBV fiber mats were initially assessed by DSC and thermogravimetric analysis (TGA). TGA showed that the additives decreased the thermal stability of PHBV in the fiber mats, except for ATBC, which showed no significant difference (Figure S2 and Table S1 in the Supporting Information). All glycerol-based additives caused the most significant decrease in thermal stability, resulting in a two-staged degradation profile. In contrast, the addition of ChCl:Urea:Water exhibited a single-stage degradation profile, showing the most prominent decrease in thermal stability across all samples. These results suggest that these additives might exhibit a prodegradative effect on PHBV, as also suggested previously.[54] By DSC, reductions in the glass transition temperature (T_g) and melting temperature (T_m) have been previously connected with a decrease in mechanical rigidity.[23,55] Therefore, it is the first heating run on the fiber mats that is relevant for this study. Cooling and second heating runs were not provided due to the degradative effects (as seen in TGA data, Figure S2, Table S1) of the additives on PHBV during prolonged thermal exposure, which could further obscure the thermal transition data. Thus, Table 2 and Figure 4 summarize the thermal transitions of as-obtained and aged electrospun PHBV fiber samples with and without additives obtained during the first run. The T_g of the PHBV fiber mats with and without additives could not be unambiguously detected by DSC.

For the samples measured immediately after electrospinning (as obtained), pure PHBV fiber mats exhibited a melting point of 173.9 °C; however, the PHBV mats containing ChCl:Gly and ChCl:Urea:Water exhibited a depression in melting point of 0.7 and 3.1 °C, respectively. Among DESs, the highest reduction in melting point was observed for the addition of Gly:NaCitrate, exhibiting a decrease of 5.6 °C in comparison to pure PHBV. A melting point decrease is related to a reduction in thickness and/or perfection of the crystalline lamella.[44]

Table 2. Thermal Parameters Obtained from First Heating for Pure PHBV, PHBV/Gly, PHBV/ATBC, and PHBV/DES Fiber Mats As Obtained and Aged: Melting Temperature (T_m) and Melting Enthalpy (ΔH_m)

samples	T_m (°C)		ΔH_m (J/g)		ΔH_m change (J/g)
	as obtained	aged	as obtained	aged	
pure PHBV	173.9	171.8	92.2	101.2	9.0
PHBV/Gly:NaCitrate	168.3	168.3	82.8	104.6	21.8
PHBV/Gly	165.7	167.2	100.2	108.6	8.4
PHBV/ChCl:Gly	173.2	171.7	82.8	89.5	6.7
PHBV/ATBC	169.0	169.4	83.2	93.7	10.5
PHBV/ChCl:Urea:Water	170.8	174.4	86.0	88.1	2.1

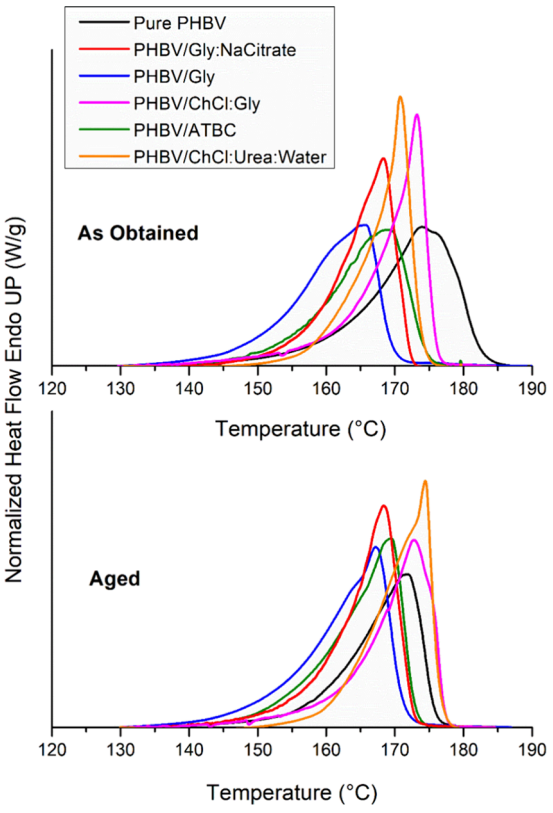

Figure 4. First melting endotherms of pure PHBV, PHBV/Gly, PHBV/ATBC and PHBV/DES fiber mats as obtained and aged.

For comparison purposes, the thermal properties of PHBV with two conventional known plasticizers, ATBC and glycerol, were also analyzed. PHBV/ATBC exhibited a melting point decrease of 4.9 °C, less than the reduction observed for the PHBV/Gly:NaCitrate fiber mats. Similar results were obtained by Martino et al., who additivated PHBV (ENMAT Y1000P) by melt extrusion with 10 wt % of ATBC, GTA, and PEG and reported that the addition of these additives reduced the melting point of PHBV by up to 6 °C.[24] Regarding glycerol, its addition into PHBV fibers exhibited the highest melting temperature reduction of 8.2 °C. Jost et al. additivated the same PHBV polymer (ENMAT Y1000P) using various plasticizers, including glycerol by the melt extrusion method, reporting a decrease in the melting point of 4 °C.[23]

The analysis by DSC was also performed in the aged materials because these polymers are known to undergo secondary crystallization over time, leading to an increase in stiffness.[16,17] Table 2 demonstrates that the initial melting temperature of pure PHBV fiber mats was 173.9 °C, and it decreased by 2.1 °C for the aged sample. As for the reduction in melting point for the aged samples, this can be attributed to the development of less perfect crystallites, which would broaden the melting peak toward lower temperatures. However, PHBV fiber mats having conventional plasticizers displayed an increase in melting temperatures by aging. PHBV/ATBC mats displayed a slight

https://doi.org/10.1021/acsomega.4c08969
ACS Omega 2025, 10, 12936−12952

melting temperature increase from 169.0 to 169.4 °C, whereas this was more significant for glycerol-containing samples by 1.5 °C.

The effect of aging was also different for the DES-containing PHBV fiber mats. Among DES, Gly:NaCitrate-containing fibers exhibited the lowest melting temperatures in both as-obtained and aged samples. Compared to these, PHBV/ChCl:Gly and PHBV/ChCl:Urea:Water fiber mats showed higher melting temperatures, with the increase being more significant for the latter. Overall, when all aged samples were compared, PHBV/Gly, PHBV/Gly:NaCitrate, and PHBV/ATBC fiber mats exhibited lower melting temperatures. Additionally, observing Figure 4, it is also possible to identify peak shoulders for some samples, namely, PHBV/ChCl:Urea:Water (aged) and PHBV/Gly (as obtained, aged), which can be ascribed to the development of different types of crystal sizes and degrees of perfection, as previously mentioned.[56,57] Another observation from the figure is that the melting endotherms of as-obtained PHBV/ChCl:Urea:Water and PHBV/ChCl:Gly are sharper compared to those of pure PHBV as well as those of Gly and ATBC-containing PHBV fibers. Meanwhile, the melting endotherm of PHBV/Gly:NaCitrate can be found at an intermediate level. A broader melting endotherm could be attributed to variations in crystal thickness, perfection, or distribution within the polymer matrix.[58,59] Later, for the aged samples, the melting endotherms appeared to be sharper.

The melting enthalpy is directly related to polymer crystallinity.[60,61] Due to secondary crystallization phenomena, the melting enthalpies (ΔH_m's) of PHBV-based fibers are expected to increase over time, implying an increase in lateral molecular order and hence rigidity.[59] As expected and shown in Table 2, pure PHBV fiber mats exhibited an increase in ΔH_m values over time, with the as-obtained samples showing a value of 92.2 J/g, which increased to 101.2 J/g after aging. This was also the case for additive-containing PHBV fiber mats exhibiting a ΔH_m value increase over time, suggesting that all samples underwent secondary crystallization phenomena.

The presence of additives can have a significant influence on ΔH_m values. For instance, whether as obtained or aged, PHBV/ATBC fiber mats exhibited lower ΔH_m values compared to those of pure PHBV. However, other studies in PHBV incorporating ATBC and utilizing melt processing methods (i.e., compression molding, extrusion, injection molding) previously reported that ATBC increased the degree of crystallinity, and thus the ΔH_m, of PHBV films.[24,46,62] In the case of the addition of pure glycerol, an opposite trend was observed, showing increased ΔH_m (108.6 J/g) values compared with the pure PHBV fiber mats. A similar phenomenon was observed by Quispe et al.,[29] who reported that thermo-compressed PHB films containing 10 wt % glycerol exhibited higher ΔH_m values than pure PHB films. This increase was attributed to the enhanced mobility of the polymer chains due to the addition of low-molecular-weight glycerol.

The influence of DES on ΔH_m demonstrated fundamental differences when compared with pure PHBV. PHBV fiber mats containing both ChCl:Gly and ChCl:Urea:Water exhibited lower ΔH_m values in as-obtained and aged samples. Interestingly, the trend was different for PHBV/Gly:NaCitrate fiber mats; they displayed a lower ΔH_m (82.8 J/g) in as-obtained samples but experienced a substantial increase of 21.8 J/g, showing a higher ΔH_m (104.6 J/g) in the aged samples. It is known that the addition of certain low-molecular-weight compatible additives can increase the enthalpy of melting of PHAs, and thus the crystallinity, due to increased chain mobility, which promotes an enhanced polymer chain packing during the aging process at room temperature.[44,63,64] For instance, Brandolt et al. plasticized injection-molded PHBV (ENMAT Y1000) with 20 wt % of triethyl citrate (TEC), reporting an increased degree of crystallization of PHBV due to the addition of TEC.[64] This effect could be attributed to the higher compatibility and increased molecular mobility caused by the addition of Gly:NaCitrate.[63,65]

Overall, based on the initial DSC assessment, it can be interpreted that the addition of pure glycerol, ATBC, and Gly:NaCitrate showed the highest impact in the thermal properties of the PHBV fibers. However, it is important to note that the thermal kinetics of PHAs are quite complex and the DSC method, which is a dynamic method, may not provide a comprehensive insight about the actual polymer crystallinity, especially in PHA polymers.[15,32] For this reason, the crystallinity of the materials was also evaluated by simultaneous WAXS and SAXS experiments.

3.5. Crystalline Structure. Simultaneous synchrotron wide-angle X-ray scattering (WAXS) and small-angle X-ray (SAXS) experiments were carried out at room temperature to further ascertain the crystalline phase alterations induced by the different DESs. For this, conventional plasticizers, i.e., glycerol and ATBC, were also incorporated into PHBV fibers. Additionally, to investigate the effect of secondary crystallization, pure PHBV fiber mats were selected and analyzed immediately after the fiber production, as represented with dashed lines in Figure 5, whereas all other mats were analyzed after aging (solid lines). All results are gathered in Figure 5 in the 2θ range of 6 to 22°. All fiber mats revealed the typical diffraction patterns of the α-form crystalline structure that can be observed for pure PHB homopolymers, which present orthorhombic crystalline lattices with a space group of $P2_12_12_1$ (D^2_4).[15] The peak at 8.75° corresponds to the (020) diffraction, and the peak at 11° corresponds to the (110) diffraction. Additionally, all samples also contained a small quantity of β-form crystals, as evidenced by the diffraction shoulder at ~13° (this will be addressed in detail later in this section).[29,57,66−68] Furthermore, only slight

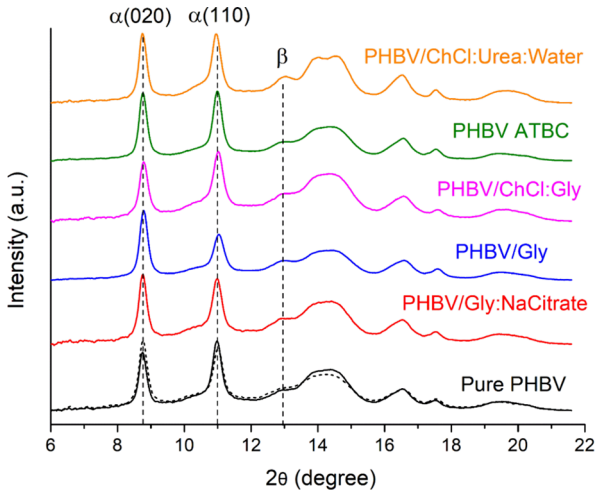

Figure 5. Normalized in intensity synchrotron wide-angle X-ray scattering (WAXS) patterns of the electrospun fiber mats of PHBV with and without the additives of different DES, Gly, and ATBC. The dashed line represents the WAXS pattern of pure PHBV fiber mats analyzed as obtained, while all other solid lines correspond to samples analyzed after aging.

https://doi.org/10.1021/acsomega.4c08969
ACS Omega 2025, 10, 12936−12952

Table 3. Unit Cell Parameters *a*, *b*, and *c*; Crystallinity; Interplanar Distances; and Crystallite Sizes for PHBV-Based Fiber Mats with and without the Additives of Different DES, Gly, and ATBC[a]

samples	PHB-like lattice (Å)			crystallinity (%)	interplanar distance (Å)		crystallite size (Å)		*R* (*β*/*α*)
	a	*b*	*c*		d020	d110	D020	D110	
pure PHBV (as obtained)	5.68	13.09	6.06	56	6.54	5.21	170.4	173.3	0.313
pure PHBV	5.70	13.10	6.00	62	6.55	5.22	183.8	183.8	0.454
PHBV/Gly:NaCitrate	5.70	13.10	6.01	57	6.55	5.22	180.9	176.0	0.512
PHBV/Gly	5.67	13.06	6.02	61	6.53	5.20	178.1	159.1	0.356
PHBV/ChCl:Gly	5.68	13.06	5.97	64	6.53	5.21	169.5	171.4	0.623
PHBV/ChCl:Urea:Water	5.71	13.10	5.94	65	6.55	5.23	187.8	193.0	0.616
PHBV/ATBC	5.69	13.09	6.00	62	6.54	5.22	185.5	187.4	0.371

[a]Only pure PHBV fiber mats were analyzed both as obtained and aged, while all other samples were analyzed in their aged condition.

peak shifts toward higher 2θ values were detected for PHBV/ChCl:Gly and PHBV/Gly fiber mats, whereas PHBV/ChCl:Urea:Water samples exhibited a slight shift toward lower 2θ values. This suggests that these additives might have caused slight alterations in the crystalline morphology of PHBV.[69]

Another observation from Figure 5 is that no additional crystalline peaks were detected in PHBV fiber mats containing ChCl:Urea:Water, ChCl:Gly, and Gly:NaCitrate. Choline chloride, urea, and sodium citrate are known to exhibit specific Bragg reflections.[70,71] The absence of these peaks suggests that these DESs did not crystallize during or after the electrospinning process.

WAXS parameters, such as unit cell parameters, crystallinity, interplanar distances, and crystallite sizes, were estimated and gathered in Table 3 for PHBV-based fiber mats with and without the additives of Gly:NaCitrate, Gly, ChCl:Gly, ChCl:Urea:-Water, and ATBC. It can be seen from the table that the additives provoked only a small difference in the unit cell parameters (*a*, *b*, and *c*). Additionally, the same trend could be observed for interplanar distances, displaying slight variations across all samples.

The degree of crystallinity of the developed PHBV-based fiber mats was also estimated from the WAXS diffractograms, and it is shown in Table 3. As-obtained pure PHBV mats exhibited a degree of crystallinity of 56%. However, when the same sample was analyzed after aging, its crystallinity was increased to 62%. This is due to the well-known secondary crystallization phenomenon of PHAs leading to an increased crystallinity over time at room temperature.[72] In the case of PHBV mats having additives, estimated overall crystallinities showed variations depending on the formulations. When ATBC and glycerol were incorporated into the polymer matrix, the crystallinity values remained similar at approximately 62%. In this context, Martino et al. observed a modest increase in estimated WAXS crystallinity by 2% for melt extruded PHBV films having 10 wt % ATBC compared to the neat films.[24] Conversely, Panaitescu et al. prepared compression molded PHB films with 5 wt % of ATBC, which resulted in a decrease in XRD crystallinity by 1.6%.[31] In the case of glycerol, Quispe et al. explored its effect on the crystallinity of thermo-compressed PHB films.[29] In their study, no decrease in XRD crystallinity was reported for the 5 wt % glycerol-containing PHB films.

Regarding PHBV fiber mats containing DES, the incorporation of ChCl-based DES led to a tiny increase in the overall crystallinity, approximately 3%, compared with pure PHBV fiber mats. Exceptionally, PHBV/Gly:NaCitrate fiber mats exhibited a somewhat decreased crystallinity, 57%, compared with the neat mats (62%). However, it is noteworthy that while the differences were not relevant, the estimated overall crystallinity values for the DES-containing PHBV fiber mats may have been underestimated to some extent. This is because there could be some contributions to the amorphous halo signal arising from the presence of liquid DES within the fibers.[73] Nevertheless, comparing the PHBV fiber mats having DES additives, the lowest estimated crystallinity was found for the PHBV/Gly:NaCitrate mats.

The apparent crystallite sizes were also estimated using the Scherrer equation (eq 1),[74] and results are shown in Table 3. As expected, pure PHBV fiber mats analyzed immediately after fiber production (as obtained) exhibited smaller crystallite sizes compared to those of the same sample but analyzed after aging. When the aged samples with conventional plasticizers were compared to the neat mats, the crystallite sizes along the (020) and (110) planes were higher in fibers containing ATBC. Conversely, in fiber mats with glycerol, there was a significant decrease in crystallite sizes on both planes. Regarding DES, both Gly:NaCitrate and ChCl:Gly provoked a decrease in crystallite sizes in both diffraction planes, whereas this was more significant for the latter. However, PHBV/ChCl:Urea:Water samples exhibited somewhat increased values, being more significant along the (110) plane. The increase in crystallite size is typically associated with more robust lateral order induced by the additives.[56,75] On the other hand, smaller crystallite sizes might be the result of the restricted PHBV chain diffusion/folding processes impaired by the presence of the additives.[76] Thus, it can be interpreted that the addition of glycerol disrupts the crystallite lattice. However, when glycerol is combined with other compounds to form DES, such as Gly:NaCitrate or ChCl:Gly, these compounds may mitigate the glycerol's disruptive effects.

Upon carefully inspecting Figure 5, it was observed that all the PHBV-based fiber mats, both with and without additives, exhibited a diffraction peak at 12.95°, which has been attributed to the so-called β-form crystals with zigzag conformations.[29,57,66−69,77] The β-form is considered to originate from the orientation of the free chains in the amorphous phase between α-form lamellar crystals.[78,79] When experiencing high stretching forces, tie molecules between the lamellar crystals will be strongly extended and oriented along the stretching direction, and thus, they would pack and form the metastable orthorhombic β-form with a planar zigzag conformation.[78] Also, several studies have revealed the occurrence of β-form morphologies in PHB or PHBV fiber mats obtained by electrospinning, in which polymers are exposed to electrostatically driven enormous stretching forces, which were then attributed to the formation of β-form structures.[77,78] For

https://doi.org/10.1021/acsomega.4c08969
ACS Omega 2025, 10, 12936−12952

instance, Chernozem et al. obtained electrospun PHB fibers containing reduced graphene oxide (rGO), and for the rGO-containing PHB fibers, they observed an increase in the Bragg reflection at 20° (when beam wavelength was 1.54 Å, corresponding to our synchrotron peak at 12.95°), which was then assigned to the zigzag conformation of the β-structure.[77] However, the crystalline structure and origin of this conformation are still under discussion and surely need additional experimental insights.[75,77] Turning our attention to our findings, as depicted in Figure 5, all electrospun fiber mats exhibited signals at the Bragg reflection of 12.95°, specifically associated with the aforementioned β-form structure. To conduct a more in-depth analysis, the relative β-form content was quantitatively assessed using the integrated intensity ratio of the β reflection to the $\alpha(020)$ reflection, as defined by Iwata et al.[79] and also applied by other others[68]. The corresponding results for each sample are compiled in Table 3. From the table, it is apparent that compared to pure PHBV, PHBV fibers containing DES consistently exhibited a higher relative β-form content. Particularly, PHBV fiber mats having ChCl-based DES showed a significantly higher β-form content. Conversely, PHBV mats having glycerol and ATBC showed the lowest values. In the morphology section, we observed thinner fibers and also long crossing thin oriented fibers. Moreover, in a prior study, we demonstrated that DES-containing PHBV fibers displayed interfiber repulsion forces arising from the polarization ability of DES, resulting in "charged" fibers.[4] Building upon this, we hypothesize that the repulsion forces between the adjacent fibers could lead fibers to experience more stretching, thereby potentially promoting the formation of β-form crystals. Additionally, the electrospinning solutions containing DES exhibited increased conductivity, which was notably more significant for the ChCl-based DES (Table 1). This heightened conductivity could lead the fibers to undergo more extensive stretching, consequently resulting in the experimentally observed higher relative β-form content.

In addition, the crystalline structure of the PHBV-based fiber mats was further characterized by SAXS. Figure 6 displays the Lorentz corrected ($I(q)q^2$) SAXS profiles of PHBV-based fiber mats, both with and without additives. As with the WAXS analysis, pure PHBV mats were examined in two states: as obtained (black dashed lines) and aged (black solid lines), whereas all other fiber samples were analyzed only in their aged state, indicated by solid lines. Observing Figure 6a, the SAXS peak for aged PHBV fiber mats exhibits a slight shift toward lower q values compared with the as-obtained PHBV sample. This suggests that aging may lead to an increase in the so-called long period, as when the sample begins upon heating to melt the more defective crystals.[32] Comparing the aged PHBV fiber mats containing additives (Figure 6b) with their neat counterpart (Figure 6a), it was observed that PHBV fibers having ATBC and ChCl:Urea:Water exhibited a significant shifts toward lower q values and the SAXS peaks became stronger compared to other samples, indicating an increase in the long period and an improved phase structure regularity.[32,80] This effect of ATBC aligns with the finding of Kurusu et al., who developed injection-molded PHB films using tributyl citrate (TBC) and triethyl citrate (TEC) as plasticizers,[19] compounds that are chemically akin to ATBC. According to their results, when the additive was introduced (TEC and TBC) into PHB, an increase in the long period values was revealed.

In contrast, the incorporation of glycerol-based additives, including pure glycerol, ChCl:Gly, and Gly:NaCitrate, into

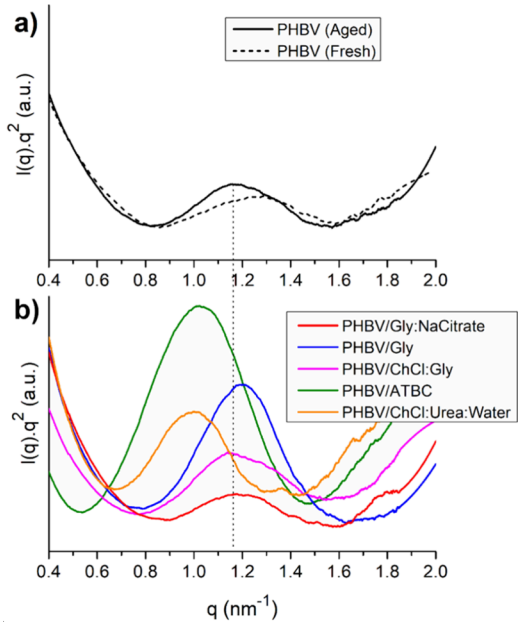

Figure 6. Lorentz corrected synchrotron small-angle X-ray scattering (SAXS) patterns of the electrospun (a) pure PHBV and (b) DES, Gly, and ATBC-containing PHBV fiber mats. Both panels a and b are presented on the same scale. Pure PHBV fiber mats were analyzed in both as-obtained and aged conditions, while all other samples were analyzed only under their aged condition.

PHBV fibers did not result in a noticeable change in the q values, which remained approximately at 1.2 nm^{-1}. This indicates that these additives did not appreciably alter the long period, which remained nearly unchanged. As suggested by Ambrosi et al.[81] and Nojima et al.,[82] SAXS curves could be described as the combined intensities originating from a two-phase structural system that includes crystalline areas and irregularities related to amorphous extralamellar domains, whereas WAXS provides insights about the overall bulk crystallinity of the samples. In WAXS analysis, it was demonstrated that the estimated overall crystallinity was within the same order of magnitude across all samples; however, the crystallite sizes of the PHBV fibers having glycerol-based additives were estimated to be smaller than those of neat PHBV, indicating potentially thinner crystalline lamellae in the modified samples, which were also observed at the lower DSC melting points. However, the irregularities in the amorphous regions could differ, as indicated by the SAXS curves. The patterns of the PHBV/Gly:NaCitrate fiber mats exhibited the most shallow peak among all samples, indicating the least ordered lamellar repeat structure.[80] Additionally, the SAXS curve of this sample, along with that of PHBV/ChCl:Urea:Water, appeared to be somewhat narrower, which might suggest less variability in repeat sizes compared to other samples.[80]

3.6. Mechanical Tests. The influence of the additives on the mechanical properties of the electrospun fiber mats was analyzed on the basis of elastic modulus (E), tensile strength at break (σ_b), elongation at break (ε_b), toughness (U), and aging.[83] The most representative tensile stress−strain curves are gathered in Figure 7, and Table 4 summarizes the mechanical property values obtained from the averaged tensile curves. Overall, it is evident from the observation of the figure that the additives exhibit significantly different behaviors across all cases. In particular, PHBV/Gly:NaCitrate fiber mats showed a very interesting and

https://doi.org/10.1021/acsomega.4c08969
ACS Omega 2025, 10, 12936−12952

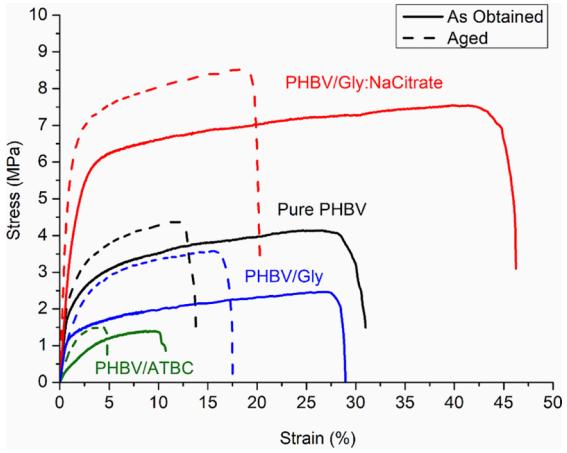

Figure 7. Tensile stress−strain curves as a function of aging time for the electrospun fiber mats: PHBV with and without additives of ATBC, Gly, and Gly:NaCitrate. Solid lines represent as-obtained samples, while dashed lines correspond to samples analyzed after aging.

unique mechanical balance between rigidity and toughness compared not only to the neat mats of PHBV but also to PHBV processed by any other methods. In contrast, PHBV fibers treated with ChCl-based DES were excessively brittle, prompting the exclusion of PHBV/ChCl:Gly and PHBV/ChCl:Urea:Water fibers from any consideration of mechanical properties.

Upon detailed examination of the as-obtained (day 0) samples, see Table 4, the neat PHBV fiber mats without additives exhibited mean values of elastic modulus (E) and tensile strength at break (σ_b) of 248 and 4 MPa, respectively, whereas the elongation at break (ε_b) and toughness (U) values were 28.1% and 0.4 mJ/mm^3, respectively. Addition of ATBC decreased the elastic modulus and tensile strength of pure PHBV fiber mats by 76 and 70% at day 0, respectively. Surprisingly, ATBC resulted also in a decrease in the elongation at break and toughness values of PHBV fiber mats by 65 and 90%, respectively, at day 0. This outcome was unexpected, as ATBC has been regarded as one of the best plasticizers for PHAs, known to enhance elongation at break when incorporated into PHBV.[62] However, in the literature, these results generally involve melt processing of PHBV and ATBC. For instance, Martino et al. studied the effect of 10 wt % ATBC in a melt extruded commercial PHBV matrix (ENMAT Y1000P),[24] which resulted in decreases of 6 °C in DSC melting point and 2% in WAXS crystallinity. Their mechanical test results showed a 36% decrease in modulus and an increase in ε_b from 1.8 to 6.4%. Similarly, Corrêa et al. produced injection molded films containing 10 wt % ATBC blended with PHBV (with 18% HV content),[62] which led to a 5 °C decrease in T_m and a 10% increase in crystallinity according to DSC analysis. They reported a 32% decrease in E and 105% increase in impact absorption capacity. Although the data on changes in elongation at break were not reported, it was noted that the ATBC-plasticized PHBV samples demonstrated good deformation at the break. In another example, concerning the plasticizing of PHBV (18% HV content) with the same concentration of ATBC via extrusion, Branciforti et al. reported a different plasticizing behavior than those mentioned immediately above.[61] In their case, the addition of ATBC caused a similar decrease in DSC melting points by 2 °C but also a decrease in DSC crystallinity by 4%, whereas the plasticizer had little to no influence on the WAXS crystallinity. Interestingly and similar to the observed mechanical performance here, ATBC reduced all mechanical properties of the PHBV films. This was attributed to the potential lack of compatibility between the components and partial phase separation. To the best of our knowledge, there is no existing data in the literature regarding the electrospinning of fibers containing ATBC in PHB or PHBV. However, Arrieta et al. reported the plasticization of electrospun PLA−PHB fiber blends using ATBC (PLA/PHB/ATBC is of 64:21:15 wt %),[84] observing a decrease in modulus and an increase in elongation at break.

The addition of glycerol caused a decrease in the elastic modulus, tensile strength, and toughness values of PHBV fiber mats. However, differently from the PHBV/ATBC mats, the elongation at the break value remained almost the same as that of pure PHBV samples. Similar to ATBC, in the literature, the plasticization of PHB and its copolymers with glycerol was generally attempted using melt processing;[23,29] however, no studies were found for the electrospinning technique. For instance, Jost et al.[23] plasticized the same grade of PHBV used in this study with 10 wt % of glycerol using melt extrusion, which reduced the DSC melting point by 4 °C and crystallinity by 6%. According to their mechanical test results, glycerol induced a plasticizing effect, resulting in a 42% decrease in elastic modulus and an increase of 38% in elongation at break values of PHBV.

Table 4. Mechanical Properties of Electrospun PHBV Fiber Mats with and without Additives of DES, Gly, and Gly:NaCitrate, in Terms of Elastic Modulus (E), Tensile Strength at Break (σ_b), Elongation at Break (ε_b), and Toughness (U), in Both As-Obtained and Aged Conditions[a]

	as obtained				aged			
sample	E (MPa)	σ_b (MPa)	ε_b (%)	U (mJ/mm^3)	E (MPa)	σ_b (MPa)	ε_b (%)	U (mJ/mm^3)
PHBV	248 ± 19^b	4.0 ± 0^b	28.1 ± 5.6^b	1 ± 0.2^b	340 ± 22^b	4.3 ± 0.1^b	12.1 ± 1.8^c	0.4 ± 0.1^b
PHBV/ATBC	60 ± 25^c	1.2 ± 0.1^d	9.9 ± 1.2^c	0.1 ± 0^b	97 ± 22^c	1.3 ± 0.3^c	4.4 ± 0.3^b	0.1 ± 0^c
% change to pure PHBV	−76%	−70%	−65%	−90%	−71%	−70%	−64%	−75%
PHBV/Gly	189 ± 15^b	2.3 ± 0.2^c	25.1 ± 8.4^b	0.5 ± 0^b	196 ± 44^c	3.6 ± 1.3^b	16.5 ± 2.2^{a,b}	0.5 ± 0.3^b
% change to pure PHBV	−24%	−43%	−11%	−50%	−42%	−16%	+36%	+25%
PHBV/Gly:NaCitrate	391 ± 82^a	7.4 ± 0.2^a	44.1 ± 4.5^a	2.9 ± 0.3^a	746 ± 64^a	8.5 ± 0.8^a	20.5 ± 2.7^a	1.6 ± 0.3^a
% change to pure PHBV	+58%	+85%	+57%	+190%	+119%	+98%	+69%	+300%
PHBV/ChCl:Gly	too brittle				too brittle			
PHBV/ChCl:Urea:Water	too brittle				too brittle			

[a]Different letters in the same column indicate a significant difference among the samples ($p < 0.05$).

https://doi.org/10.1021/acsomega.4c08969
ACS Omega 2025, 10, 12936−12952

Among the tested DESs, the PHBV fibers added with Gly:NaCitrate showed the most promising results. Unlike the ChCl-based DESs, which led to excessive brittleness, the addition of Gly:NaCitrate significantly improved all mechanical properties of the PHBV fiber mats. Compared to the as-obtained pure PHBV fiber mats, PHBV/Gly:NaCitrate mats exhibited an increase in elastic modulus, tensile strength, and elongation at break values by 58, 85, and 57%, respectively (see Table 4). Moreover, the toughness of PHBV/Gly:NaCitrate fiber mats was 190% higher than that of pure PHBV mats due to the fact that these samples exhibit higher modulus and elongation at break, hence requiring more energy before fracture. The observed increases in all mechanical properties suggest the simultaneous influence of reinforcing factors (as seen in the increased E and σ_b) and plasticizing effects (indicated by the increased ε_b).

Finally, to investigate the well-known secondary crystallization effect,[19,85] the mechanical properties of PHBV-based fiber mats with and without plasticizers were analyzed after aging. The results are visualized in Figure 7 by the dashed lines and are summarized in Table 4. As expected, when the samples were aged, pure PHBV mats exhibited a reduction in elongation at break accompanied by an increase in both elastic modulus and tensile strength. This embrittlement behavior over time was similarly observed for the PHBV mats containing 10 wt % of the various additives. In all cases, the elongation at break values of PHBV mats containing additives were roughly halved after 1 week, whereas the values of elastic modulus and tensile strength increased. However, among all samples, the aged PHBV/Gly:NaCitrate fiber mats still exhibited the highest changes compared to pure PHBV mats, with increases of 119% in E, 98% in σ_b, 69% for ε_b, and a remarkable 300% in the toughness. In any case, these changes provide clear evidence that all fiber samples still underwent secondary crystallization, consequently leading to embrittlement.

At this point, it is relevant to realize that the mechanical properties are the result of several structural and morphological factors. During the electrospinning process, changes in the structural properties of the fibers, such as crystallinity, mat homogeneity, fiber morphology, interfiber cross-linking, and orientation, play a significant role in the physical deformation behavior of the fiber mats.[37,86−88] As elucidated in the review paper by Baji et al., the application of high shear and elongation forces during fiber formation facilitates the alignment of macromolecular chains along the fiber axis, thereby inducing a pronounced degree of molecular orientation.[37] This alignment of molecular chains is anticipated to enhance the tensile strength and modulus of the fibers.[37,86,88] As can be expected from the higher conductivities of DES-containing electrospinning solutions and also demonstrated in our previous work, DES-containing PHBV fibers experience more stretching and become thinner during the electrospinning process due to the increased conductivity and also the polarization ability of DES, thus resulting in higher molecular orientation. This mechanism likely contributes to the observed superior mechanical strength in PHBV/DES fiber mats, particularly those with ChCl-based DES. Conversely, PHBV fiber mats containing only glycerol or ATBC exhibited the opposite effect as these substances did not show increased conductivity and produced more random, thicker, and highly cross-linked fibers. Another great potential of the electrospinning process is its ability to enable unique nonwoven morphological features. For instance, the elongation at break for the PHBV used containing 2−3% 3HV content when processed using conventional melt-compounding methods is typically limited to a maximum of 4%, as confirmed by both the literature[23,32−34] and the manufacturer.[89] Conversely, the elongation at break values obtained here for the same PHBV grade reached as high as 28% in the as-obtained pure PHBV fibers, whereas it was 12% for the aged one. This enhancement can be attributed to the processing method's ability to stretch polymer chains under high elongation rates while solidifying very rapidly, effectively handicapping the formation of thick crystalline lamellae and leading to reduced crystallinity.[37] Another morphological effect on the tensile properties is interfiber bonding leading to cross-linked self-standing structures. Interfiber bonding is known to improve the elastic modulus and ultimate tensile strength of the fiber mats, whereas a reduced bonding allows for easier orientation and stretching during tensile loading, potentially resulting in a high degree of elongation before failure.[37] As seen in Figure 2, PHBV/Gly:NaCitrate fibers appeared to exhibit the least cross-linked and homogeneous mat morphology compared with other samples. The latter effect could be one of the reasons for its highest elongation at break values. Additionally, porosity could potentially influence the mechanical properties of fiber mats. Typically, fiber mats with a lower porosity, characterized by a higher fiber density, are expected to demonstrate higher stiffness and strength compared to their more porous counterparts.[40,86] Furthermore, when the mat porosity is low, the interfiber bonding is more effective for increasing the stiffness.[40] Thus, the relatively higher porosity and lesser interfiber bonding of PHBV/Gly:NaCitrate may account for its increased stretchability.

In addition, as previously discussed and visually represented in Figure 2, PHBV/ATBC fibers exhibited a fractured morphology with notable heterogeneity in fiber thickness, ranging from remarkably thick to exceedingly thin. This could also contribute to the earlier mechanical failure of the PHBV/ATBC fiber mats. Finally, it was observed from Figure 3 that pure glycerol- and DES-containing PHBV fibers exhibited nanovoids along the fiber surface. In this regard, some studies suggest that nanoholes may lead to lower mechanical strength.[90,91] Conversely, other research indicates that nanoholes can act as stress concentrators during deformation, significantly enhancing strain through a "nanonecking" mechanism.[92,93] In any case, here, the nanovoids are thought to contain the liquid glycerol and DES phases, which could act if homogeneously dispersed as lubricants to assist the stretching of the polymer.

The crystalline content and morphology are also known to have an influence on mechanical properties.[60,85] As discussed earlier, the overall WAXS crystallinities of PHBV-based samples were found to fluctuate by only 5% between samples, with PHBV/Gly:NaCitrate fiber mats having the lowest crystallinity of 57%. Therefore, discussing the effect of the overall crystallinity on mechanical performance becomes somewhat challenging. Nevertheless, the PHBV/Gly:NaCitrate-containing mat showed the highest reduction in the melting point and weak SAXS patterns. Moreover, it is worth noting that the generation of β-form crystals, which was discussed in the previous section, could significantly contribute to the mechanical properties, including tensile strength, elastic modulus, and elongation at break.[78,79,94] In this context, Iwata and colleagues produced PHB films and fibers that exhibited remarkable mechanical characteristics.[79,95,96] They indicated that the presence of β-form crystals played a pivotal role in augmenting the mechanical

https://doi.org/10.1021/acsomega.4c08969
ACS Omega 2025, 10, 12936−12952

properties. Later, in more recent studies, this was also observed by other authors, reporting better mechanical properties attributed to the β-form structures.[68,75] Based on this, when comparing the PHBV fiber mats containing DES, the highest overall WAXS crystallinity and relative β-form content were observed for the fibers having ChCl-based DES, whereas PHBV/Gly:NaCitrate fiber mats showed somewhat lower crystallinity but higher β-form content compared to pure PHBV mats. Hence, this may contribute to the observed excessive brittleness in PHBV/ChCl:Gly and PHBV/ChCl:Urea:Water fiber mats, alongside the comprehensive improvement in all mechanical parameters of the PHBV/Gly:NaCitrate sample.

Another factor that could influence the tensile behavior of the fiber mats is the potential chemical interactions between PHBV and the additives. In fact, ATR-FTIR spectroscopy was performed on the developed PHBV-based fiber mats to investigate this, and the results are presented in Figure S3 of the Supporting Information. According to the results, no new features, band shifts, or shape changes were unambiguously detected in the fingerprint region (1400−600 cm^{-1}) or in the carbonyl group band (C═O, 1720 cm^{-1}),[97] suggesting no chemical alterations on the PHBV. The only observation was a clear peak shift toward higher wavenumbers in the −OH stretching region (3600−3000 cm^{-1}) of DES and pure glycerol, which suggests a weakening of the hydrogen bonding strength[98] of the additives in the mat compared to its pure liquid state, maybe as a result of the reduced size filling the nanovoids. Although no detectable chemical alterations were observed by ATR-FTIR spectroscopy, the compatibility of compounds is thought to benefit the mechanical behavior. Compatibility is the ability of an additive to form a homogeneous system with the polymer with high miscibility, which influences the mechanical behavior.[99] As discussed earlier and seen in the literature, sodium citrate and ATBC, both citrates, are expected to be compatible with PHBV.[19,21,23−27] Glycerol was also utilized as a PHBV plasticizer before, showing some favorable softening effects,[23,29] as we also observed in this study. On the other hand, no reports have suggested the possible compatibility between PHAs and choline chloride and/or urea. In the case of ATBC, although it is known as a PHA-compatible additive, its observed mechanical failure can be attributed to its particular heterogeneous and thicker fiber mat morphology. Finally, regarding the observed remarkable mechanical improvements with the addition of Gly:NaCitrate, the compatibility with PHBV could potentially arise from the physicochemical properties of their individual components. Sodium citrate, with its citrate backbone, may exhibit some favorable compatibilization effect to PHBV, enhancing the polymer's flexibility. Glycerol, known for its softening effects on PHBV, could further improve its mechanical performance during deformation by reducing the intermolecular forces within the polymer matrix. These combined effects likely play a favorable role during mechanical deformation.

4. CONCLUSIONS

The present study was aimed at investigating the performance of various DES formulations on modulating the mechanical properties of electrospun PHBV mats. Thus, for the first time, several DESs, i.e., ChCl:Urea:Water, ChCl:Gly, and Gly:NaCitrate, were formulated and loaded into electrospun PHBV fibers at a concentration of 10 wt % with respect to the polymer. For comparative purposes, conventional plasticizers, namely, glycerol and ATBC, were also evaluated at identical concentration levels. All samples produced macroscopically consistent, self-supporting, and handleable nonwoven material sheets. Morphological characterizations revealed that both pure PHBV and PHBV/ATBC fibers displayed a partially fused, highly interconnected, and smoother fiber morphology with an average fiber diameter of 1200 and 860 nm, respectively. Additionally, the latter samples also displayed broken fibers and the highest porosity. On the other hand, DES-containing PHBV fiber mats resulted in thinner and rugous fiber morphologies in the size range of around 650 nm. Within the mats containing DES, the one with PHBV/Gly:NaCitrate exhibited the most homogeneous morphology with apparently less fiber interconnecting points. Glycerol and DES rugose morphologies suggest that the filler is very finely dispersed and has distributed segregated domains across the fibers. Differential scanning calorimetry (DSC) analysis was carried out on both as-obtained and aged samples to evaluate the influence of DES on the thermal behavior of the PHBV fiber mats. Among DESs, Gly:NaCitrate showed the lowest melting temperature, whereas ChCl-based DES exhibited higher melting temperatures. Simultaneous synchrotron WAXS and SAXS analysis was carried out on the samples. The incorporation of Gly:NaCitrate exhibited slightly lower WAXS crystallinity, whereas ChCl-based DES provoked an increase in the PHBV crystallinity. Additionally, electrospun PHBV fiber mats containing DES showed a higher relative β-crystal content compared to pure PHBV, PHBV/ATBC, and PHBV/Gly samples, which was higher for the ChCl-based DES. The mechanical performance of the various mat materials was very different. Surprisingly, PHBV/Gly:NaCitrate fiber mats showed a remarkable unreported increase in all mechanical properties, including elastic modulus, tensile strength, elongation at break, and toughness, compared to the PHBV polymer. The unique behavior of this material was ascribed to the particular morphology exhibited by the mat, high β-form crystal content, higher compatibility with the biopolymer, lower melting point, and more ill-defined repeat structure at the mesoscale.

In this work, the impact of DES addition on mechanical properties was evaluated through its effects on crystallinity, morphology, mat homogeneity, porosity, and thermal properties. Despite this comprehensive evaluation, the fundamental mechanisms underlying these modifications—commonly referred to as plasticization—remained not fully understood, with several theories proposed but none fully explaining all observed effects. To bridge this gap, future research will focus on elucidating the interaction between DES and PHAs, particularly their influence on physicochemical properties, to broaden the applicability of these materials in various fields. Additionally, these studies must address chemical safety concerns through overall and specific migration tests, which are crucial for determining the suitability and long-term stability of these materials for potential applications such as food packaging, agriculture, medicine, and pharmaceuticals.

Overall, this study represents the pioneering application of the DES technology to influence the mechanical properties of electrospun fiber mats based on PHBV by using the electrospinning technique. It showcases the remarkable versatility and efficiency of DES in modifying the electrospun PHBV properties, positioning it as a viable, sustainable, and cost-effective alternative for balancing the PHBV's properties.

https://doi.org/10.1021/acsomega.4c08969
ACS Omega 2025, 10, 12936−12952

■ ASSOCIATED CONTENT

Supporting Information

The Supporting Information is available free of charge at https://pubs.acs.org/doi/10.1021/acsomega.4c08969.

Additional experimental details, methods, and characterizations of PHBV fiber mats with and without additives of ATBC, Gly, Gly:NaCitrate, ChCl:Gly, ChCl:Urea:Water include thermogravimetric analysis (TGA) and attenuated total reflectance Fourier transformed infrared (ATR-FTIR) spectroscopy (PDF)

■ AUTHOR INFORMATION

Corresponding Authors

Cristina Prieto − *Novel Materials and Nanotechnology group, Institute of Agrochemistry and Food Technology (IATA), Spanish Council for Scientific Research (CSIC), Paterna 46980, Spain;* orcid.org/0000-0002-0925-896X; Phone: (+34) 963 900 022; Email: cprieto@iata.csic.es

Jose M. Lagaron − *Novel Materials and Nanotechnology group, Institute of Agrochemistry and Food Technology (IATA), Spanish Council for Scientific Research (CSIC), Paterna 46980, Spain;* orcid.org/0000-0002-0502-359X; Phone: (+34) 963 900 022; Email: lagaron@iata.csic.es

Authors

Ahmet O. Basar − *Novel Materials and Nanotechnology group, Institute of Agrochemistry and Food Technology (IATA), Spanish Council for Scientific Research (CSIC), Paterna 46980, Spain*

Luis Cabedo − *Polymers and Advanced Materials Group (PIMA), Universitat Jaume I (UJI), Castelló de la Plana 12071, Spain;* orcid.org/0000-0002-3361-6579

Complete contact information is available at: https://pubs.acs.org/10.1021/acsomega.4c08969

Author Contributions

A.O.B.: contributed to the formal analysis, investigation, writing of the original draft, and visualization. C.P: contributed to the conceptualization, methodology, editing draft, and supervision. L.C.: contributed to the investigation. J.M.L: contributed to the conceptualization, methodology, resources, editing draft, supervision, project administration, and funding acquisition.

Funding

This work was supported by the MICIN/AEI/10.13039/501100011033 and by "ERDF A way of making Europe" [project PID2021-128749OB-C31] and the ALBA Synchrotron, Barcelona, Spain [project 2021095319].

Notes

The authors declare no competing financial interest.

■ ACKNOWLEDGMENTS

A.O. Basar wants to thank the Generalitat Valenciana (GVA) for his Grisolía PhD Fellowship (GRISOLIA/2020/19). The authors would like to acknowledge the Polymer Technology joint unit CSIC-UJI, the CSIC-PTI SusPlast, and the accreditation as Center of Excellence Severo Ochoa CEX2021-001189-S funded by MCIU/AEI/10.13039/501100011033.

■ REFERENCES

(1) Abbott, A. P.; Capper, G.; Davies, D. L.; Rasheed, R. K.; Tambyrajah, V. Novel Solvent Properties of Choline Chloride/Urea Mixtures. *Chem. Commun.* **2003**, *1*, 70−71.

(2) Martins, M. A. R.; Pinho, S. P.; Coutinho, J. A. P. Insights into the Nature of Eutectic and Deep Eutectic Mixtures. *J. Solution Chem.* **2019**, *48* (7), 962−982.

(3) Hansen, B. B.; Spittle, S.; Chen, B.; Poe, D.; Zhang, Y.; Klein, J. M.; Horton, A.; Adhikari, L.; Zelovich, T.; Doherty, B. W.; Gurkan, B.; Maginn, E. J.; Ragauskas, A.; Dadmun, M.; Zawodzinski, T. A.; Baker, G. A.; Tuckerman, M. E.; Savinell, R. F.; Sangoro, J. R. Deep Eutectic Solvents: A Review of Fundamentals and Applications. *Chem. Rev.* **2021**, *121* (3), 1232−1285.

(4) Basar, A. O.; Prieto, C.; Pardo-Figuerez, M.; Lagaron, J. M. Poly(3-Hydroxybutyrate-Co-3-Hydroxyvalerate) Electrospun Nanofibers Containing Natural Deep Eutectic Solvents Exhibiting a 3D Rugose Morphology and Charge Retention Properties. *ACS Omega* **2023**, *8*, 3798.

(5) Svigelj, R.; Dossi, N.; Grazioli, C.; Toniolo, R. Deep Eutectic Solvents (Dess) and Their Application in Biosensor Development. *Sensors* **2021**, *21* (13), 4263.

(6) Abranches, D. O.; Coutinho, J. A. P. Everything You Wanted to Know about Deep Eutectic Solvents but Were Afraid to Be Told. *Annu. Rev. Chem. Biomol. Eng.* **2023**, *14*, 141−163.

(7) Cunha, S. C.; Fernandes, J. O. Extraction Techniques with Deep Eutectic Solvents. *TrAC - Trends Anal. Chem.* **2018**, *105*, 225−239.

(8) García, G.; Aparicio, S.; Ullah, R.; Atilhan, M. Deep Eutectic Solvents: Physicochemical Properties and Gas Separation Applications. *Energy Fuels* **2015**, *29* (4), 2616−2644.

(9) Smith, E. L.; Abbott, A. P.; Ryder, K. S. Deep Eutectic Solvents (DESs) and Their Applications. *Chem. Rev.* **2014**, *114* (21), 11060−11082.

(10) Sirviö, J. A.; Visanko, M.; Ukkola, J.; Liimatainen, H. Effect of Plasticizers on the Mechanical and Thermomechanical Properties of Cellulose-Based Biocomposite Films. *Ind. Crops Prod.* **2018**, *122* (June), 513−521.

(11) Adamus, J.; Spychaj, T.; Zdanowicz, M.; Jędrzejewski, R. Thermoplastic Starch with Deep Eutectic Solvents and Montmorillonite as a Base for Composite Materials. *Ind. Crops Prod.* **2018**, *123* (January), 278−284.

(12) Sokolova, M. P.; Smirnov, M. A.; Samarov, A. A.; Bobrova, N. V.; Vorobiov, V. K.; Popova, E. N.; Filippova, E.; Geydt, P.; Lahderanta, E.; Toikka, A. M. Plasticizing of Chitosan Films with Deep Eutectic Mixture of Malonic Acid and Choline Chloride. *Carbohydr. Polym.* **2018**, *197* (June), 548−557.

(13) Yilmaz, M. T.; Kul, E.; Saricaoglu, F. T.; Odabas, H. I.; Taylan, O.; Dertli, E. Deep Eutectic Solvent as Plasticizing Agent for the Zein Based Films. *Food Packag. Shelf Life* **2024**, *42* (October 2023), No. 101252.

(14) Sabapathy, P. C.; Devaraj, S.; Meixner, K.; Anburajan, P.; Kathirvel, P.; Ravikumar, Y.; Zabed, H. M.; Qi, X. Recent Developments in Polyhydroxyalkanoates (PHAs) Production − A Review. *Bioresour. Technol.* **2020**, *306* (March), No. 123132.

(15) Melendez-Rodriguez, B.; Reis, M. A. M.; Carvalheira, M.; Sammon, C.; Cabedo, L.; Torres-Giner, S.; Lagaron, J. M. Development and Characterization of Electrospun Biopapers of Poly(3-Hydroxybutyrate- Co-3-Hydroxyvalerate) Derived from Cheese Whey with Varying 3-Hydroxyvalerate Contents. *Biomacromolecules* **2021**, *22* (7), 2935−2953.

(16) Kelly, C. A.; Fitzgerald, A. V. L.; Jenkins, M. J. Control of the Secondary Crystallisation Process in Poly(Hydroxybutyrate-Co-Hydroxyvalerate) through the Incorporation of Poly(Ethylene Glycol). *Polym. Degrad. Stab.* **2018**, *148* (September 2017), 67−74.

(17) Srubar, W. V.; Wright, Z. C.; Tsui, A.; Michel, A. T.; Billington, S. L.; Frank, C. W. Characterizing the Effects of Ambient Aging on the Mechanical and Physical Properties of Two Commercially Available Bacterial Thermoplastics. *Polym. Degrad. Stab.* **2012**, *97* (10), 1922−1929.

(18) Barbosa, J. L.; Perin, G. B.; Felisberti, M. I. Plasticization of Poly(3-Hydroxybutyrate- Co-3-Hydroxyvalerate) with an Oligomeric Polyester: Miscibility and Effect of the Microstructure and Plasticizer Distribution on Thermal and Mechanical Properties. *ACS Omega* **2021**, *6* (4), 3278−3290.
(19) Kurusu, R. S.; Siliki, C. A.; David, É.; Demarquette, N. R.; Gauthier, C.; Chenal, J. M. Incorporation of Plasticizers in Sugarcane-Based Poly(3-Hydroxybutyrate)(PHB): Changes in Microstructure and Properties through Ageing and Annealing. *Ind. Crops Prod.* **2015**, *72*, 166−174.
(20) Righetti, M. C.; Aliotta, L.; Mallegni, N.; Gazzano, M.; Passaglia, E.; Cinelli, P.; Lazzeri, A. Constrained Amorphous Interphase and Mechanical Properties of Poly (3-Hydroxybutyrate- Co −3- Hydroxyvalerate). *Front. Chem.* **2019**, *7* (November), 1−16.
(21) Erceg, M.; Kovačić, T.; Klarić, I. Thermal Degradation of Poly(3-Hydroxybutyrate) Plasticized with Acetyl Tributyl Citrate. *Polym. Degrad. Stab.* **2005**, *90* (2 SPEC. ISS), 313−318.
(22) Immergut, E. H.; Mark, H. F.Principles of Plasticization. In *Plasticization and Plasticizer Processes*; American Chemical Society: Washington, DC, 1965; pp 1−26. .
(23) Jost, V.; Langowski, H. C. Effect of Different Plasticisers on the Mechanical and Barrier Properties of Extruded Cast PHBV Films. *Eur. Polym. J.* **2015**, *68*, 302−312.
(24) Martino, L.; Berthet, M. A.; Angellier-Coussy, H.; Gontard, N. Understanding External Plasticization of Melt Extruded PHBV-Wheat Straw Fibers Biodegradable Composites for Food Packaging. *J. Appl. Polym. Sci.* **2015**, *132* (10), 1−11.
(25) Choi, J. S.; Park, W. H. Effect of Biodegradable Plasticizers on Thermal and Mechanical Properties of Poly(3-Hydroxybutyrate). *Polym. Test.* **2004**, *23* (4), 455−460.
(26) Slongo, M. D.; Brandolt, S. D. F.; Daitx, T. S.; Mauler, R. S.; Giovanela, M.; Crespo, J. S.; Carli, L. N. Comparison of the Effect of Plasticizers on PHBV—and Organoclay—Based Biodegradable Polymer Nanocomposites. *J. Polym. Environ.* **2018**, *26* (6), 2290−2299.
(27) Wang, L.; Zhu, W.; Wang, X.; Chen, X.; Chen, G.-Q.; Xu, K. Processability Modifications of Poly(3-Hydroxybutyrate) by Plasticizing, Blending, and Stabilizing. *J. Appl. Polym. Sci.* **2008**, *107* (1), 166−173.
(28) Grillo Fernandes, E.; Pietrini, M.; Chiellini, E. Thermo-Mechanical and Morphological Characterization of Plasticized Poly-[(R)-3-Hydroxybutyric Acid]. *Macromol. Symp.* **2004**, *218*, 157−164.
(29) Quispe, M. M.; Lopez, O. V.; Boina, D. A.; Stumbé, J. F.; Villar, M. A. Glycerol-Based Additives of Poly(3-Hydroxybutyrate) Films. *Polym. Test.* **2021**, *93*, No. 107005.
(30) Nosal, H.; Moser, K.; Warzała, M.; Holzer, A.; Stańczyk, D.; Sabura, E. Selected Fatty Acids Esters as Potential PHB-V Bioplasticizers: Effect on Mechanical Properties of the Polymer. *J. Polym. Environ.* **2021**, *29* (1), 38−53.
(31) Panaitescu, D. M.; Nicolae, C. A.; Frone, A. N.; Chiulan, I.; Stanescu, P. O.; Draghici, C.; Iorga, M.; Mihailescu, M. Plasticized Poly(3-Hydroxybutyrate) with Improved Melt Processing and Balanced Properties. *J. Appl. Polym. Sci.* **2017**, *134*, 19, .
(32) Melendez-Rodriguez, B.; Torres-Giner, S.; Lorini, L.; Valentino, F.; Sammon, C.; Cabedo, L.; Lagaron, J. M. Valorization of Municipal Biowaste into Electrospun Poly(3-Hydroxybutyrate-Co-3-Hydroxyvalerate) Biopapers for Food Packaging Applications. *ACS Appl. Bio Mater.* **2020**, *3* (9), 6110−6123.
(33) Javadi, A.; Srithep, Y.; Pilla, S.; Lee, J.; Gong, S.; Turng, L. S. Processing and Characterization of Solid and Microcellular PHBV/Coir Fiber Composites. *Mater. Sci. Eng., C* **2010**, *30* (5), 749−757.
(34) Martínez-Abad, A.; González-Ausejo, J.; Lagarón, J. M.; Cabedo, L. Biodegradable Poly(3-Hydroxybutyrate-Co-3-Hydroxyvalerate)/Thermoplastic Polyurethane Blends with Improved Mechanical and Barrier Performance. *Polym. Degrad. Stab.* **2016**, *132*, 52−61.
(35) Figueroa-Lopez, K. J.; Enescu, D.; Torres-Giner, S.; Cabedo, L.; Cerqueira, M. A.; Pastrana, L.; Fuciños, P.; Lagaron, J. M. Development of Electrospun Active Films of Poly(3-Hydroxybutyrate-Co-3-Hydroxyvalerate) by the Incorporation of Cyclodextrin Inclusion Complexes Containing Oregano Essential Oil. *Food Hydrocoll.* **2020**, *108*, No. 106013.
(36) Liu, Y.; Hao, M.; Zhou, C.; Yang, B.; Jiang, S.; Huang, J.; Chen, Z.; Liu, Y.; Ramakrishna, S.Scale-up Strategies for Electrospun Nanofiber Production. In *Electrospun and Nanofibrous Membranes, Principles and Applications:*1*Edition;*Kargari, A., Matsuura, T., Shirazi, M. M. A., Ed.; Elsevier Inc, 2022; pp 205−266. .
(37) Baji, A.; Mai, Y. W.; Wong, S. C.; Abtahi, M.; Chen, P. Electrospinning of Polymer Nanofibers: Effects on Oriented Morphology, Structures and Tensile Properties. *Compos. Sci. Technol.* **2010**, *70* (5), 703−718.
(38) Bensalem, Z.; Chabane, H.; Ababsa, H. S.; Mekki, A.; Livi, S. Ionic Liquids versus Deep Eutectic Solvent: A Tunable Platform for the Design of Biopolymer Blends. *ACS Sustain. Chem. Eng.* **2024**, *12* (3), 1309−1319.
(39) Delamarche, E.; Mattlet, A.; Livi, S.; Gérard, J. F.; Bayard, R.; Massardier, V. Tailoring Biodegradability of Poly(Butylene Succinate)/Poly(Lactic Acid) Blends With a Deep Eutectic Solvent. *Front. Mater.* **2020**, *7* (February), 1−13.
(40) Wang, Y.; Ma, C.; Liu, C.; Lu, X.; Feng, X.; Ji, X. Thermodynamic Study of Choline Chloride-Based Deep Eutectic Solvents with Water and Methanol. *J. Chem. Eng. Data* **2020**, *65* (5), 2446−2457.
(41) Jancheva, M.; Grigorakis, S.; Loupassaki, S.; Makris, D. P. Optimised Extraction of Antioxidant Polyphenols from Satureja Thymbra Using Newly Designed Glycerol-Based Natural Low-Transition Temperature Mixtures (LTTMs). *J. Appl. Res. Med. Aromat. Plants* **2017**, *6*, 31−40.
(42) Chavoshnejad, P.; Razavi, M. J. Effect of the Interfiber Bonding on the Mechanical Behavior of Electrospun Fibrous Mats. *Sci. Rep.* **2020**, *10* (1), 1−11.
(43) Werker, A.; Pei, R.; Kim, K.; Moretto, G.; Estevez-Alonso, A.; Vermeer, C.; Arcos-Hernandez, M.; Dijkstra, J.; de Vries, E. Thermal Pre-Processing before Extraction of Polyhydroxyalkanoates for Molecular Weight Quality Control. *Polym. Degrad. Stab.* **2023**, *209* (January), No. 110277.
(44) Jenkins, M. J.; Robbins, K. E.; Kelly, C. A. Secondary Crystallisation and Degradation in P(3HB-Co-3HV): An Assessment of Long-Term Stability. *Polym. J.* **2018**, *50* (5), 365−373.
(45) Biddlestone, F.; Harris, A.; Hay, J. N.; Hammond, T. The Physical Ageing of Amorphous Poly(Hydroxybutyrate). *Polym. Int.* **1996**, *39* (3), 221−229.
(46) Brdlík, P.; Borůvka, M.; Běhálek, L.; Lenfeld, P. The Influence of Additives and Environment on Biodegradation of PHBV Biocomposites. *Polymers (Basel).* **2022**, *14* (4), 838.
(47) Zdanowicz, M.; Wilpiszewska, K.; Spychaj, T. Deep Eutectic Solvents for Polysaccharides Processing. A Review. *Carbohydr. Polym.* **2018**, *200* (July), 361−380.
(48) Xue, J.; Wu, T.; Dai, Y.; Xia, Y. Electrospinning and Electrospun Nanofibers: Methods, Materials, and Applications. *Chem. Rev.* **2019**, *119* (8), 5298−5415.
(49) Wagner, A.; Poursorkhabi, V.; Mohanty, A. K.; Misra, M. Analysis of Porous Electrospun Fibers from Poly(l-Lactic Acid)/Poly(3-Hydroxybutyrate-Co-3-Hydroxyvalerate) Blends. *ACS Sustain. Chem. Eng.* **2014**, *2* (8), 1976−1982.
(50) Zuo, W.; Zhu, M.; Yang, W.; Yu, H.; Chen, Y.; Zhang, Y. Experimental Study on Relationship between Jet Instability and Formation of Beaded Fibers during Electrospinning. *Polym. Eng. Sci.* **2005**, *45* (5), 704−709.
(51) Choi, J. S.; Lee, S. W.; Jeong, L.; Bae, S. H.; Min, B. C.; Youk, J. H.; Park, W. H. Effect of Organosoluble Salts on the Nanofibrous Structure of Electrospun Poly(3-Hydroxybutyrate-Co-3-Hydroxyvalerate). *Int. J. Biol. Macromol.* **2004**, *34* (4), 249−256.
(52) Abbott, A. P.; Harris, R. C.; Ryder, K. S.; D'Agostino, C.; Gladden, L. F.; Mantle, M. D. Glycerol Eutectics as Sustainable Solvent Systems. *Green Chem.* **2011**, *13* (1), 82−90.
(53) Angammana, C. J.; Jayaram, S. H. Analysis of the Effects of Solution Conductivity on Electrospinning Process and Fiber Morphology. *IEEE Trans. Ind. Appl.* **2011**, *47* (3), 1109−1117.

https://doi.org/10.1021/acsomega.4c08969
ACS Omega 2025, 10, 12936−12952

(54) Janigová, I.; Lacík, I.; Chodák, I. Thermal Degradation of Plasticized Poly(3-Hydroxybutyrate) Investigated by DSC. *Polym. Degrad. Stab.* **2002**, *77* (1), 35−41.
(55) Wypych, G.Effect of Plasticizers on Properties of Plasticized Materials. In *Handbook of Plasticizers*; Wypych, G., Ed.; ChemTec Publishing: Toronto, 2017; pp 209−332. .
(56) Righetti, M. C.; Di Lorenzo, M. L. Melting Temperature Evolution of Non-Reorganized Crystals. Poly(3-Hydroxybutyrate). *Thermochim. Acta* **2011**, *512* (1−2), 59−66.
(57) Frone, A. N.; Nicolae, C. A.; Eremia, M. C.; Tofan, V.; Ghiurea, M.; Chiulan, I.; Radu, E.; Damian, C. M.; Panaitescu, D. M. Low Molecular Weight and Polymeric Modifiers as Toughening Agents in Poly(3-hydroxybutyrate) Films. *Polymers (Basel).* **2020**, *12* (11), 2446.
(58) Ding, C.; Cheng, B.; Wu, Q. DSC Analysis of Isothermally Melt-Crystallized Bacterial Poly(3-Hydroxybutyrate-Co-3-Hydroxyhexanoate) Films. *J. Therm. Anal. Calorim.* **2011**, *103* (3), 1001−1006.
(59) Hu, Y.; Zhang, J.; Sato, H.; Noda, I.; Ozaki, Y. Multiple Melting Behavior of Poly(3-Hydroxybutyrate-Co-3-Hydroxyhexanoate) Investigated by Differential Scanning Calorimetry and Infrared Spectroscopy. *Polymer (Guildf).* **2007**, *48* (16), 4777−4785.
(60) Auriemma, F.; Alfonso, G. C.; de Rosa, C.*Polymer Crystallization I, From Chain Microstructure to Processing*, First.; Auriemma, F., Alfonso, G. C., de Rosa, C., Eds.; Springer Cham, 2005; Vol. *37*. .
(61) Branciforti, M. C.; Corrêa, M. C. S.; Pollet, E.; Agnelli, J. A. M.; Nascente, P. A. D. P.; Avérous, L. Crystallinity Study of Nano-Biocomposites Based on Plasticized Poly(Hydroxybutyrate-Co-Hydroxyvalerate) with Organo-Modified Montmorillonite. *Polym. Test.* **2013**, *32* (7), 1253−1260.
(62) Corrêa, M. C. S.; Branciforti, M. C.; Pollet, E.; Agnelli, J. A. M.; Nascente, P. A. P.; Avérous, L. Elaboration and Characterization of Nano-Biocomposites Based on Plasticized Poly(Hydroxybutyrate-Co-Hydroxyvalerate) with Organo-Modified Montmorillonite. *J. Polym. Environ.* **2012**, *20* (2), 283−290.
(63) Lopera-Valle, A.; Caputo, J. V.; Leão, R.; Sauvageau, D.; Luz, S. M.; Elias, A. Influence of Epoxidized Canola Oil (ECO) and Cellulose Nanocrystals (CNCs) on the Mechanical and Thermal Properties of Polyhydroxybutyrate (PHB)-Poly(Lactic Acid) (PLA) Blends. *Polymers (Basel).* **2019**, *11* (6), 933.
(64) Brandolt, S. D. F.; Daitx, T. S.; Mauler, R. S.; Ornaghi Junior, H. L.; Crespo, J. S.; Carli, L. N. Synergistic Effect between Different Clays and Plasticizer on the Properties of PHBV Nanocomposites. *Polym. Compos.* **2019**, *40* (10), 3835−3843.
(65) Jun, D.; Guomin, Z.; Mingzhu, P.; Leilei, Z.; Dagang, L.; Rui, Z. Crystallization and Mechanical Properties of Reinforced PHBV Composites Using Melt Compounding: Effect of CNCs and CNFs. *Carbohydr. Polym.* **2017**, *168*, 255−262.
(66) de Sousa Junior, R. R.; dos Santos, C. A. S.; Ito, N. M.; Suqueira, A. N.; Lackner, M.; dos Santos, D. J. PHB Processability and Property Improvement with Linear-Chain Polyester Oligomers Used as Plasticizers. *Polymers (Basel).* **2022**, *14* (19), 4197.
(67) Mottin, A. C.; Ayres, E.; Oréfice, R. L.; Câmara, J. J. D. What Changes in Poly(3-Hydroxybutyrate) (PHB) When Processed as Electrospun Nanofibers or Thermo-Compression Molded Film? *Mater. Res.* **2016**, *19* (1), 57−66.
(68) Yang, J.; Zhu, H.; Zhao, Y.; Jiang, Q.; Chen, H.; Liu, G.; Chen, P.; Wang, D. New Insights into the Beta-Form Crystal Toughening Mechanism in Pre-Oriented PHBV Films. *Eur. Polym. J.* **2017**, *91* (October 2016), 81−91.
(69) Zhao, X.; Cornish, K.; Vodovotz, Y. Synergistic Mechanisms Underlie the Peroxide and Coagent Improvement of Natural-Rubber-Toughened Poly(3-Hydroxybutyrate-Co-3-Hydroxyvalerate) Mechanical Performance. *Polymers* **2019**, *11* (3), 565.
(70) Yuan, C.; Chu, K.; Li, H.; Su, L.; Yang, K.; Wang, Y.; Li, X. In Situ Raman and Synchrotron X-Ray Diffraction Study on Crystallization of Choline Chloride/Urea Deep Eutectic Solvent under High Pressure. *Chem. Phys. Lett.* **2016**, *661*, 240−245.
(71) Gao, J.; Wang, Y.; Hao, H. Investigations on Dehydration Processes of Trisodium Citrate Hydrates. *Front. Chem. Sci. Eng.* **2012**, *6* (3), 276−281.
(72) Eraslan, K.; Aversa, C.; Nofar, M.; Barletta, M.; Gisario, A.; Salehiyan, R.; Goksu, Y. A. Poly(3-Hydroxybutyrate-Co-3-Hydroxyhexanoate) (PHBH): Synthesis, Properties, and Applications - A Review. *Eur. Polym. J.* **2022**, *167* (November 2021), No. 111044.
(73) Depoorter, J.; Mourlevat, A.; Sudre, G.; Morfin, I.; Prasad, K.; Serghei, A.; Bernard, J.; Fleury, E.; Charlot, A. Fully Biosourced Materials from Combination of Choline Chloride-Based Deep Eutectic Solvents and Guar Gum. *ACS Sustain. Chem. Eng.* **2019**, *7* (19), 16747−16756.
(74) Shaalan, N. M.; Hamad, D.; Abdel-Latief, A. Y.; Abdel-Rahim, M. A. Preparation of Quantum Size of Tin Oxide: Structural and Physical Characterization. *Prog. Nat. Sci. Mater. Int.* **2016**, *26* (2), 145−151.
(75) Yang, J.; Liu, X.; Zhao, J.; Pu, X.; Shen, Z.; Xu, W.; Liu, Y. The Structural Evolution of β-to-α Phase Transition in the Annealing Process of Poly(3-Hydroxybutyrate-Co-3-Hydroxyvalerate). *Polymers* **2023**, *15* (8), 1921.
(76) Zhang, H.; Yu, H. Y.; Wang, C.; Yao, J. Effect of Silver Contents in Cellulose Nanocrystal/Silver Nanohybrids on PHBV Crystallization and Property Improvements. *Carbohydr. Polym.* **2017**, *173*, 7−16.
(77) Chernozem, R. V.; Romanyuk, K. N.; Grubova, I.; Chernozem, P. V.; Surmeneva, M. A.; Mukhortova, Y. R.; Wilhelm, M.; Ludwig, T.; Mathur, S.; Kholkin, A. L.; Neyts, E.; Parakhonskiy, B.; Skirtach, A. G.; Surmenev, R. A. Enhanced Piezoresponse and Surface Electric Potential of Hybrid Biodegradable Polyhydroxybutyrate Scaffolds Functionalized with Reduced Graphene Oxide for Tissue Engineering. *Nano Energy* **2021**, *89* (PB), No. 106473.
(78) Gong, L.; Chase, D. B.; Noda, I.; Liu, J.; Martin, D. C.; Ni, C.; Rabolt, J. F. Discovery of β-Form Crystal Structure in Electrospun Poly[(R)-3-Hydroxybutyrate-Co-(R)-3-Hydroxyhexanoate] (PHBHx) Nanofibers: From Fiber Mats to Single Fibers. *Macromolecules* **2015**, *48* (17), 6197−6205.
(79) Kabe, T.; Tsuge, T.; Kasuya, K. I.; Takemura, A.; Hikima, T.; Takata, M.; Iwata, T. Physical and Structural Effects of Adding Ultrahigh-Molecular-Weight Poly[(R)-3-Hydroxybutyrate] to Wild-Type Poly[(R)-3-Hydroxybutyrate]. *Macromolecules* **2012**, *45* (4), 1858−1865.
(80) Lagaron, J. M.; Vickers, M. E.; Powell, A. K.; Bonner, J. G. On the Effect of the Nature of the Side Chain over the Crystalline Structure in Aliphatic Polyketones. *Polymer (Guildf).* **2002**, *43* (6), 1877−1886.
(81) Ambrosi, M.; Raudino, M.; Diañez, I.; Martínez, I. Non-Isothermal Crystallization Kinetics and Morphology of Poly(3-Hydroxybutyrate)/Pluronic Blends. *Eur. Polym. J.* **2019**, *120* (June), 109189.
(82) Nojima, S.; Terashima, Y.; Ashida, T. Small-Angle X-Ray Scattering Study of the Morphology of Blends of Poly(ϵ-Caprolactone) and Polystyrene Oligomer. *Polymer (Guildf).* **1986**, *27* (7), 1007−1013.
(83) Wypych, G.Plasticizer Motion and Diffusion: Plasticizer Distribution in Materials in Contact. In *Handbook of Plasticizers:3E-dition*; Wypych, G., Ed.; ChemTec Publishing: Toronto, 2017; pp 165−186. .
(84) Arrieta, M. P.; López, J.; López, D.; Kenny, J. M.; Peponi, L. Biodegradable Electrospun Bionanocomposite Fibers Based on Plasticized PLA−PHB Blends Reinforced with Cellulose Nanocrystals. *Ind. Crops Prod.* **2016**, *93*, 290−301.
(85) Wang, Q.; Xu, Y.; Xu, P.; Yang, W.; Chen, M.; Dong, W.; Ma, P. Crystallization of Microbial Polyhydroxyalkanoates: A Review. *Int. J. Biol. Macromol.* **2022**, *209* (PA), 330−343.
(86) Aghjeh, M. K. R.; Razavi, M. J.Effect of Interfibre Bonding on Mechanical Behaviour of Electrospun Fibrous Mats. In *Mechanics of Fibrous Networks*; Silberschmidt, V., Ed.; Elsevier Ltd., 2022; pp 317−354. .
(87) Wu, T.; Li, H.; Xue, J.; Mo, X.; Xia, Y. Photothermal Welding, Melting, and Patterned Expansion of Nonwoven Mats of Polymer Nanofibers for Biomedical and Printing Applications. *Angew. Chemie - Int. Ed.* **2019**, *58* (46), 16416−16421.
(88) Arinstein, A.; Burman, M.; Gendelman, O.; Zussman, E. Effect of Supramolecular Structure on Polymer Nanofibre Elasticity. *Nat. Nanotechnol.* **2007**, *2* (1), 59−62.

https://doi.org/10.1021/acsomega.4c08969
ACS Omega 2025, 10, 12936−12952

(89) Properties, T. M.; Gravity, S.; Index, M. F.*Technical Data Sheet & Processing Guide, ENMAT PHBV resin Y1000P*. https://29475285.s21i.faiusr.com/61/ABUIABA9GAAgsIG-pQYonrPIrgc.pdf (accessed 2024−05−28). ENMAT Y1000P.
(90) Huang, L.; Bui, N. N.; Manickam, S. S.; McCutcheon, J. R. Controlling Electrospun Nanofiber Morphology and Mechanical Properties Using Humidity. *J. Polym. Sci., Part B: Polym. Phys.* **2011**, *49* (24), 1734−1744.
(91) Huan, S.; Liu, G.; Cheng, W.; Han, G.; Bai, L. Electrospun Poly(Lactic Acid)-Based Fibrous Nanocomposite Reinforced by Cellulose Nanocrystals: Impact of Fiber Uniaxial Alignment on Microstructure and Mechanical Properties. *Biomacromolecules* **2018**, *19* (3), 1037−1046.
(92) Kim, G. M.; Lach, R.; Michler, G. H.; Chang, Y. W. The Mechanical Deformation Process of Electrospun Polymer Nanocomposite Fibers. *Macromol. Rapid Commun.* **2005**, *26* (9), 728−733.
(93) Kim, G. M.; Michler, G. H.; Pötschke, P. Deformation Processes of Ultrahigh Porous Multiwalled Carbon Nanotubes/Polycarbonate Composite Fibers Prepared by Electrospinning. *Polymer (Guildf).* **2005**, *46* (18), 7346−7351.
(94) Antipov, E. M.; Dubinsky, V. A.; Rebrov, A. V.; Nekrasov, Y. P.; Gordeev, S. A.; Ungar, G. Strain-Induced Mesophase and Hard-Elastic Behaviour of Biodegradable Polyhydroxyalkanoates Fibers. *Polymer (Guildf).* **2006**, *47* (15), 5678−5690.
(95) Iwata, T.; Tsunoda, K.; Aoyagi, Y.; Kusaka, S.; Yonezawa, N.; Doi, Y. Mechanical Properties of Uniaxially Cold-Drawn Films of Poly([R]-3-Hydroxybutyrate). *Polym. Degrad. Stab.* **2003**, *79* (2), 217−224.
(96) Iwata, T.; Fujita, M.; Aoyagi, Y.; Doi, Y.; Fujisawa, T. Time-Resolved X-Ray Diffraction Study on Poly[(R)-3-Hydroxybutyrate] Films during Two-Step-Drawing: Generation Mechanism of Planar Zigzag Structure. *Biomacromolecules* **2005**, *6* (3), 1803−1809.
(97) El-Hadi, A. M. Improvement of the Miscibility by Combination of Poly(3-Hydroxy Butyrate) PHB and Poly(Propylene Carbonate) PPC with Additives. *J. Polym. Environ.* **2017**, *25* (3), 728−738.
(98) Gaweł, B. A.; Ulvensøen, A.; Łukaszuk, K.; Arstad, B.; Muggerud, A. M. F.; Erbe, A. Structural Evolution of Water and Hydroxyl Groups during Thermal, Mechanical and Chemical Treatment of High Purity Natural Quartz. *RSC Adv.* **2020**, *10* (48), 29018−29030.
(99) Senichev, V. Y.; Tereshatov, V. V.Theories of Compatibility. In *Handbook of Plasticizers:3Edition*; Wypych, G., Ed.; ChemTec Publishing: Toronto, 2017; pp 135−164. .

https://doi.org/10.1021/acsomega.4c08969
ACS Omega 2025, 10, 12936−12952